NPS-61Md72051A

NAVAL POSTGRADUATE SCHOOL

Monterey, California

15 May 1972 NPS-61Md72051A

Frequency Dependence of Sound Transmitted From An Airborne Source Into The Ocean

H. Medwin &
R.A. Helbig

Ocean Physics Group
Physics Department

NAVAL POSTGRADUATE SCHOOL
Monterey, California

Rear Admiral A.S. Goodfellow
Superintendent

M.U. Clauser
Provost

TITLE: Frequency Dependence of Sound Transmitted From An Airborne Source Into the Ocean

ABSTRACT:

The predicted dependence of sound transmission on the statistics of the randomly-rough interface between dissimilar fluids has been studied by use of the Helmholtz Integral (J. Acoust. Soc. Amer. 51, 1083-1090 (1972)). The predictions have been verified for radiation from a helicopter hovering, and slowly moving, over the sea, for frequencies to 1000 Hz for a wide range of surface acoustical roughnesses, $R = k_2^2\sigma^2[(c_2/c_1)\cos\theta_1-\cos\theta_2]^2$. The roughness parameters σ,k,c and θ are the rms height of the surface, propagation constant, speed of propagation and angle with the normal, respectively; subscript 1 refers to air and 2 to the water.

When the surface is mirror-smooth, the transmitted sound pressure is due to the change in divergence and change in impedance at the interface. For low roughness, $R < 1$, the mean square transmitted pressure becomes decreasingly coherent and is a function of frequency; its magnitude is decreased by the factor e^{-R} compared to the perfectly smooth surface. For $R \geq 1$ the incoherent component dominates and the transmitted pressure depends also on the correlation length of the surface displacements.

The transmission change of sound pressure as a function of frequency is presented for several conditions of an SH3-D helicopter hovering and flying over or near an array of microphone and sonobuoy hydrophones.

This task was supported by: Codes ASW 21, ASW 24 and the Office of Naval Research Code 468

TABLE OF CONTENTS

ACKNOWLEDGEMENTS

The authors are indebted to several people who helped in this research: to W. Smith, electronics technician who was so exceptionally effective during all aspects of the program, and to T. Maris, R. Moeller and M. Andrews, machinists at the Naval Postgraduate School; to Mrs. R.S. Lande and Mrs. P.H. Auyong who did the computer programming (NPS).

A debt of gratitude is due also to many people at Scripp's Institution of Oceanography including: Dr. Fred Spiess, Director of the Marine Physical Laboratory, and Dr. Victor Anderson, Assistant Director, for their cooperation in making the services of "FLIP" available for this project; Mr. Earl Bronson, MPL Marine Coordinator, Captain Richard A. Silva and the crew of "FLIP" for their complete cooperation and assistance during the ocean experiments; Dr. Russ Davis and Mr. Lloyd Regier for the collection and analysis of ocean surface data; Mr. Rick Ackerman and Mr. Joe Percy (NUC, San Diego) for their assistance in obtaining equipment for the experiments.

We appreciate the cooperation of personnel of Helicopter Squadron 4 at N.A.S. Imperial Beach who provided aircraft for use as sound sources.

The financial support of U.S. Navy Codes ASW 21 and ASW 24 and the Office of Naval Research (Code 468) made this research possible.

I. THEORY

The Helmholtz Integral has been used, together with the Kirchhoff Assumption, to predict the dependence of the coherent (phase cancelled) component, and the incoherent component of airborne sound transmitted through a randomly rough ocean surface[1]. The solution is given simply in terms of the rms height, σ, and the correlation length, L, of the surface. The development is very similar to that used by many others [2-7] to study the scattering of sound from a rough surface.

Reference (1) describes various forms of the problem. We summarize these results by using square brackets [] to repeat the appropriate equations of that work. We recall the cases:

A) Infinite Plane Waves Incident on a Smooth Plane Interface in which the transmitted pressure ratio at the surface is,

$$T = \frac{p_{2s}}{p_{1s}} = 1 + \frac{\rho_2 c_2/\cos\theta_2 - \rho_1 c_1/\cos\theta_1}{\rho_2 c_2/\cos\theta_2 + \rho_1 c_1/\cos\theta_1} = 1 + R \qquad [3]$$

subscripts 1 refer to the medium of incidence.

2 refer to the medium of transmission.

θ = angle measured with normal

ρ = density

c = speed of sound

p_{1s} = acoustic pressure, incident from medium 1, at the surface

p_{2s} = acoustic pressure, in medium 2, at the surface

R = pressure reflection ratio for plane waves

T = pressure transmission ratio for plane waves

B) Aperture-limited Plane Waves Incident on a Smooth Plane Interface (see Fig. 1) for which the Helmholtz Kirchhoff solution for a large aperature ($\Delta A >> \lambda$) is given by equation [6a]:

$$p_2 = \frac{1}{4\pi} \int_S \left(p \frac{\partial \psi}{\partial n} - \psi \frac{\partial p}{\partial n} \right) dS \qquad [5]$$

$$= p_{2m} \frac{F}{\Delta A} \int_{-Y}^{Y} \int_{-X}^{X} e^{i\vec{K}\cdot\vec{r}} \, dxdy \qquad [6]$$

$$= p_{2m} F \operatorname{sinc} K_x X \operatorname{sinc} K_y Y$$

where

$$p_{2m} = \left| \frac{-i2p_{10}k_2 e^{ik_2 r_2}}{4\pi r_2} \Delta A \cos \Theta_2 \right|$$

$$\Delta A = 4XY$$

$$\psi = \frac{e^{ik_2 r_2'}}{r_2'} = \frac{e^{-k_2 r_2}}{r_2} e^{-i\vec{k}_2\cdot\vec{r}}$$

$r = i_1 x + i_2 y + i_3 \zeta$, the radius vector to the surface element

r_1 = distance from source to origin of ensonified area

r_1' = distance from source to surface element

r_2 = distance from origin of ensonified area to receiver

r_2' = distance from surface element to receiver

$$\operatorname{sinc} K_x X = \frac{\sin K_x X}{K_x X}$$

$$F = 1 + \frac{(c_2/c_1 \sin \Theta_1 - \sin \Theta_2) \tan \Theta_2 \cos \Theta_3}{c_2/c_1 \cos \Theta_1 - \cos \Theta_2} \quad \frac{\sin \Theta_2 \tan \Theta_2 \sin^2 \Theta_3}{c_2/c_1 \cos \Theta_1 - \cos \Theta_2}$$

$p_{10} = \frac{p_{1A}}{r_1} e^{i(k_1 r_1 - \omega t)}$, incident acoustic pressure at surface origin

p_{1A} = acoustic pressure at unit distance from source

p_2 = acoustic pressure at the receiver

$dS = dxdy/\cos \gamma$, area of a surface element

$\zeta = \zeta(x,y)$, surface height at (x,y)

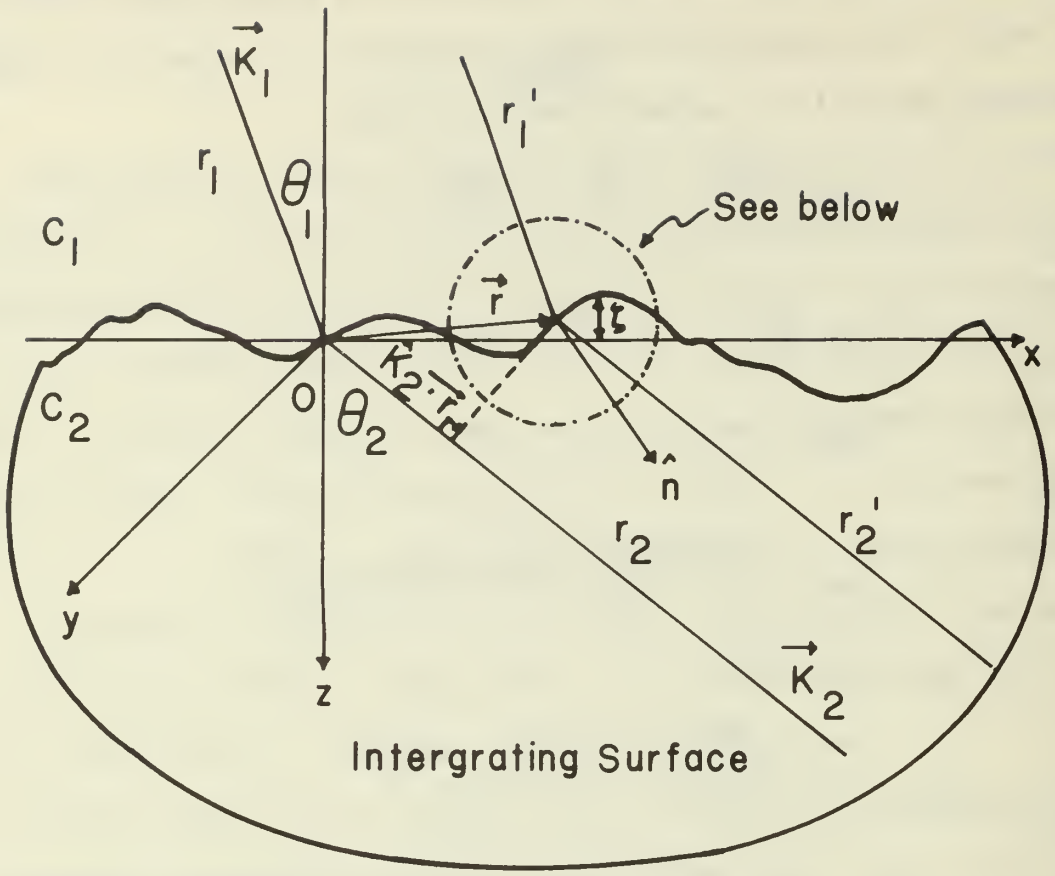

GEOMETRY OF THE PROBLEM

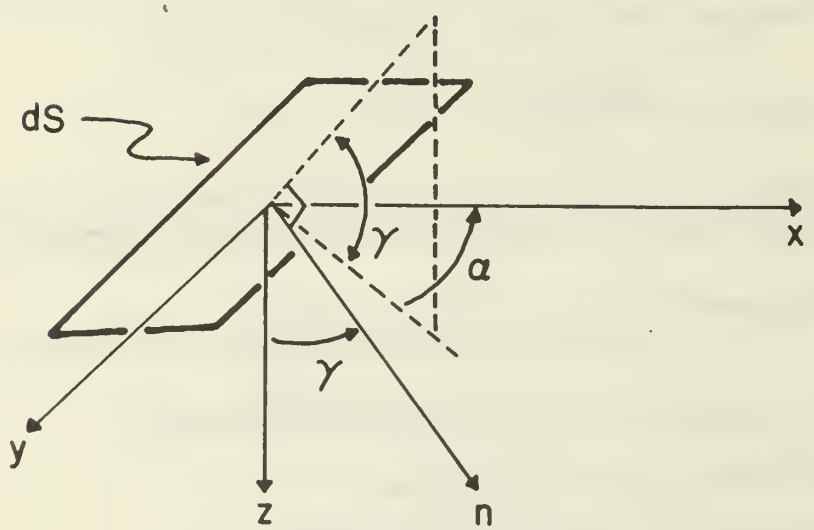

Figure 1. Geometry for Helmholtz-Kirchhoff theory for transmission of a plane wave through a randomly rough interface betwee two dissimilar media.

$\hat{n}$ = $\hat{i}_1(-\sin\gamma\cos\alpha) + \hat{i}_2(-\sin\gamma\sin\alpha) + \hat{i}_3\cos\gamma$, normal to surface element

γ = angle the normal makes with the z axis

α = angle the projection of the normal onto the xy-plane makes with the x axis

$\vec{k}_1 = \frac{2\pi f}{c_1}(\hat{i}_1\sin\theta_1 + \hat{i}_3\cos\theta_1)$, vector propagation constant of incident field

$\vec{k}_2 = \frac{2\pi f}{c_2}(\hat{i}_1\sin\theta_2\cos\theta_3 + \hat{i}_2\sin\theta_2\sin\theta_3 + \hat{i}_3\cos\theta_2)$, vector propagation constant of received field

θ_1 = angle of incidence, measured from normal to interface

θ_2 = angle that $\vec{k}_2$ makes with the z-axis

θ_3 = angle that $\vec{k}_2$ makes with the xz-plane

$\vec{K} = \vec{k}_1 - \vec{k}_2 = \hat{i}_1K_x + \hat{i}_2K_y + \hat{i}_3K_z$

$K_x = k_1\sin\theta_1 = k_2\sin\theta_2\cos\theta_3$

$K_y = k_2\sin\theta_2\sin\theta_3$

$K_z = k_1\cos\theta_1 - k_2\cos\theta_2$

$K_{xy} = (K_x^2 + K_y^2)^{\frac{1}{2}}$

C) Aperture-limited Plane Waves Incident on a Rough Plane Interface (Gaussian PDF of heights, Gaussian correlation function) for which the Helmholtz-Kirchhoff solution is given by

$$\frac{\langle p_2 p_2^* \rangle}{(p_{2m})^2} = e^{-R}F^2\,\mathrm{sinc}^2 K_xX\,\mathrm{sinc}^2 K_yY + F^2\frac{\pi L^2}{\Delta A}e^{-R}\sum_{n=1}^{\infty}\frac{R^n}{nn!}e^{-K_{xy}^2L^2/4n} \qquad [10]$$

where $R = K_z^2\sigma^2$ = acoustical roughness for transmission

$= k_2^2\sigma^2(c_2/c_1\cos\theta_1 - \cos\theta_2)^2$ [8]

σ = rms height of surface

D) Radiation From a Point Source in Air Incident on a Smooth Plane Air-water Interface, for which the sound pressure transmission change for the mirror surface, TC_M (referred to p_{1s}) is

$$TC_M = 20 \log_{10} \frac{p_{2m}}{p_{1s}} = - 20 \log_{10} \left[\left(1 + \frac{D}{H} \frac{c_2 \cos \theta_1}{c_1 \cos \theta_2} \right) \left(2 \cos\theta_1 \cos\theta_2 \right)^{-1} \right] \quad [14a]$$

where D = depth = perpendicular distance from receiver to interface

H = height = perpendicular distance from source to interface

p_{2m} = pressure at Snell angle θ_2 depth D, for a mirror-like surface, and for which the change referenced to the incident pressure at ground zero (p_{12}) is given by

$$TC_{MZ} = TC_M - 20 \log_{10} \cos \theta_1 \quad [14b]$$

E) Radiation From a Point Source in Air, Incident on a Randomly-rough Plane Air-water Interface.

This last problem is, needless to say, the most difficult. The approximate approach derived in Reference 1 and used here (Section III-C-3) is similar to that in Reference 7. The ensonified area is divided into subareas; then all the coherent contributions and, separately, all the incoherent contributions, are added. The often incompatible criteria for each subarea are: 1) the incident pressure is approximately constant and the spatial variation of the incident phase is negligible (e.g. less than $\lambda/8$) over the sub-area; 2) the linear dimension of the subarea is several surface correlation lengths in extent; 3) the correlation length is much greater than the acoustical wave length. The desirability of assumption (1) in adapting the plane wave solution is obvious. Assumption (2) states that the infinite integration that yields [10] is accomplished after "enough" correlation distances so that the spatial correlation has reached a "small" value. We will say more about this later (Section III-C-3). Assumption (3) is the requirement for our use of the Kirchhoff Assumption, in which the infinite plane wave impedance relation at the surface is assumed on a point-by-point basis.

For the point source we therefore start with Eq. [10] for the transmission through an element of area ΔA which we now call A_i, multiply by (p_{2mi}^2/p_{1si}^2), and generalize by writing the sum for many such areas, (see Fig. 2).

$$\sum_i \frac{\langle p_{2i} p_{2i}^* \rangle}{p_{1si}^2} = \sum_i \frac{p_{2mi}^2}{p_{1si}^2} e^{-R_i} F_i^2 \operatorname{sinc}^2 K_{xi} X_i \operatorname{sinc}^2 K_{yi} Y_i +$$

$$\sum_i \frac{p_{2mi}^2}{p_{1si}^2} \frac{F_i^2 \pi L^2}{A_i} e^{-R_i} \sum_{n=1}^{\infty} \frac{R_i^n}{nn!} e^{-K_{xyi}^2 L^2/4n} \qquad [15]$$

We will assign i = 1 to the terms along the Snell (ray acoustic) direction and for simplicity we drop the subscript 1 for this most important direction.

An approximate solution to the problem is obtained if we assume that there is no cross-coupling between coherent and incoherent components from each subarea. Then our problem becomes one of separately evaluating the terms

$$\frac{\langle p_2 p_2^* \rangle}{p_{1s}^2} = \frac{\langle p_{2s} \rangle^2}{p_{1s}^2} + \frac{\text{Var}\{p_{2s}\}}{p_{1s}^2} \qquad [16]$$

where the two terms on the rhs of Eq. [16] represent the respective sums of coherent and incoherent terms on the rhs of Eq. [15].

The first term of Eq. [15] is a sum of coherent components; the relative coherent transmission along the Snell direction is

$$\frac{\langle p_{2s} \rangle^2}{p_{1s}^2} \simeq e^{-R} \left(1 + \frac{Dc_2 \cos\theta_1}{Hc_1 \cos\theta_2} \right)^{-2} (2 \cos\theta_1 \cos\theta_2)^2. \qquad [17]$$

The incoherent term is obtained by summing the effects of the sub-areas. Adding this to the coherent term, and taking 10 $\log_{10}$,

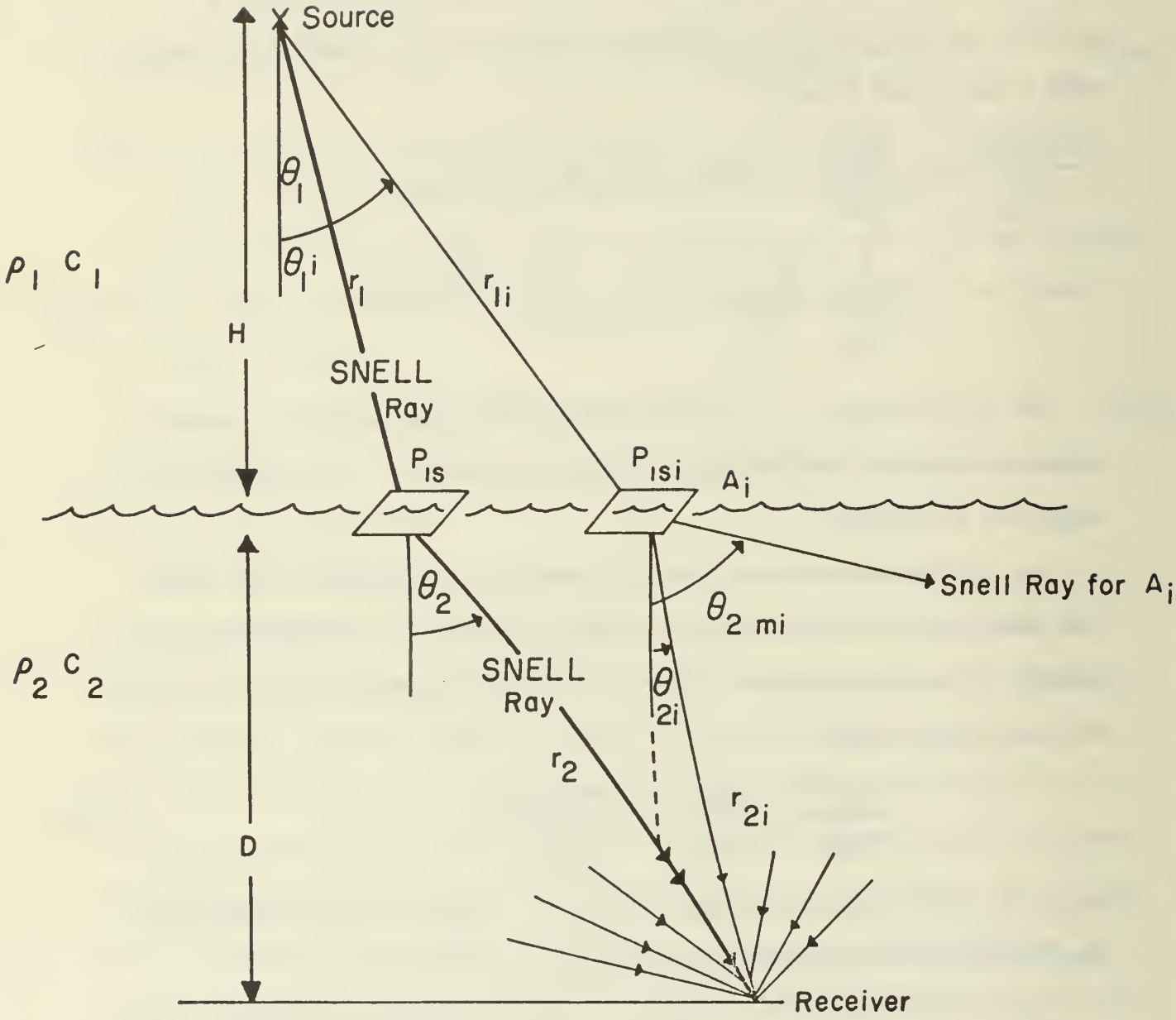

Geometry for point source above a rough surface.

Figure 2. Geometry for Helmholtz-Kirchhoff theory applied to essentially plane sub-areas of a diverging wave as it passes through a randomly rough interface between two dissimilar media.

yields

$$TC = 10 \log_{10} \frac{\langle p_{2s} p_{2s}^* \rangle}{p_{1s}^2} = 10 \log_{10} \left\{ e^{-R} \left(1 + \frac{Dc_2 \cos\theta_1}{Hc_1 \cos\theta_2} \right)^{-2} (2 \cos\theta_1 \cos\theta_2)^2 \right.$$

$$\left. + \sum_i \frac{\pi A_i L^2 \cos^2\theta_{2mi} F_i^2 S(R_i K_{xy} L)}{\lambda_2^2 r_{2i}^2 (\cos\theta_1 / \cos\theta_{1i})^2} \right\} \qquad [20]$$

where the quantities F_i and $S(R_i, K_{xy}L)$ are functions of the angles at the area element, θ_{1i} and θ_{2i} (see Fig. 2 and Reference 1).

Equation [20] states that, for very low frequencies ($R \ll 1$), the summation (incoherent) term will be very small, $e^{-R} \simeq 1$, and the transmission change will be given by the geometry and ρc mismatch, (Eq. [14]. This pressure change may be positive or negative, i.e. a transmission gain or loss, respectively. As the frequency (and roughness) increases in the regime $0 < R < 1$, the coherent transmission term will decrease but will still dominate the incoherent. For $R \rightarrow 1$, the increasing incoherent term will begin to determine the magnitude of TC in Eq. [20]. This will cause an <u>increase</u> in transmitted pressure until a high enough frequency is reached (value depending on L/λ_2) for the $S(R, K_{xy}L)$ term to decrease with frequency and to again cause a greater transmission loss.

II. <u>EXPERIMENT</u>

A series of laboratory studies were undertaken as a prelude to an experiment using a SH3D helicopter as a noise source over the sea. The laboratory results and two graphs of the ocean data have been included in a paper titled "Spectral Characteristics of Sound Transmission Through the Rough Sea Surface", by H. Medwin, R.A. Helbig and J.D. Hagy, Jr., which has been submitted for publication in the Journal of the

Acoustical Society of America (estimated publication date Dec 1972). This technical report contains the complete presentation of the transmission results of the sea trials.

The point source theory for a rough interface, Eq. [20], was tested by experiments at sea using the geometry as shown in Figs. 3 and 4. The "point" source was a Sikorsky SH-3D helicopter, at various heights, hovering or slowly moving on command over or near, an array of one microphone and several hydrophones, on command. The signal from the receivers was carried by cable to the nearby Floating Instrument Platform, FLIP, operated by the staff of the Scripps Institution of Oceanography. SCRIPPS scientists made measurements of the sea surface height spectrum, concurrently with this experiment.

Two series of experiments were conducted. FLIPEX I on 28, 29 May 1970 and FLIPEX II on 17, 18 August 1970 both at a deep sea location, 45 miles NW of San Diego. Only the results of FLIPEX II have been processed.

A. Experimental Details

The SH3-D helicopter, viewed as a sound source, is characterized by a large number of strong harmonics of the very low frequency blade passage tone of the rotor, harmonics of the high speed counter-rotation tail propellor, and a broad band aerodynamic and machinery noise spectrum, in which the harmonics are partially immersed. Only helicopter heights of 300 ft or greater are reported here; hovers at lower levels disturbed the sea surface and precluded comparison with theory.

The hydrophones were parts of modified AN/SSQ-57 sonobuoys. The two modifications consisted of: a) disabling the RF modulator, which is normally used to radio the signal from the buoy; and b) changing the length of the hydrophone support so that it hung at depth 0 (or 10 ft),

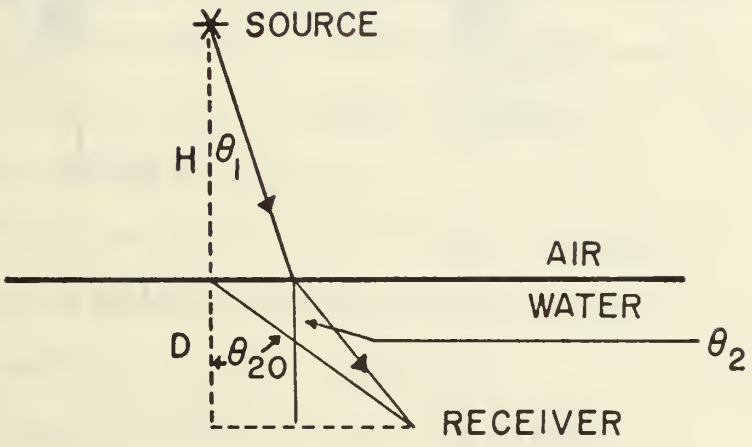

Figure 3. Geometry of transmission into water from point source in air. The Snell ray is indicated. (Not to scale.)

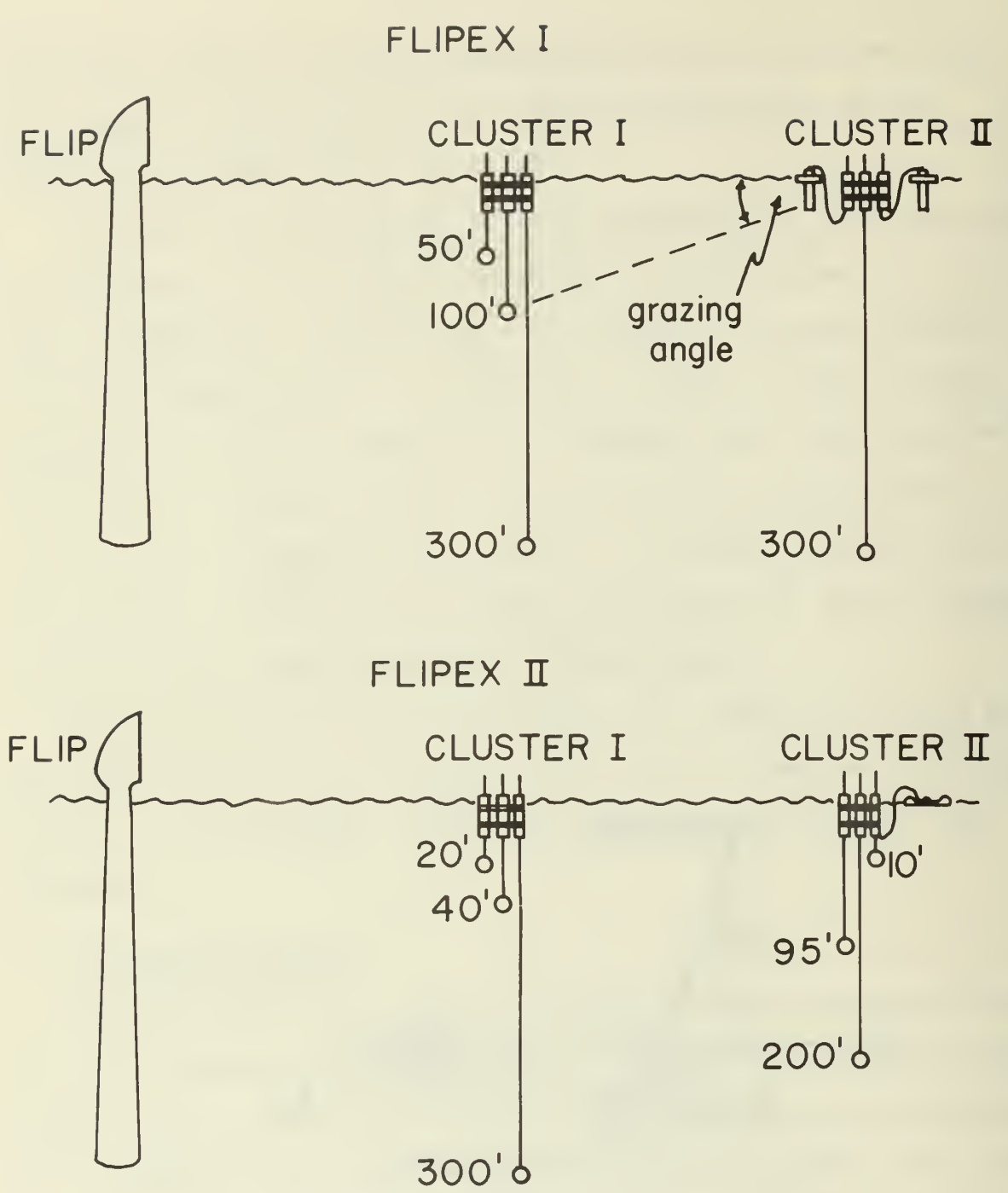

Figure 4. Experimental arrangement for ocean experiment. Noise source hovered over, or moved slowly past either Cluster I or Cluster II. For FLIPEX II, reported here, the clusters were separated by 150 ft. Ocean and acoustic data were recorded at Scripps Institutions Research Platform FLIP, 300 ft upwind from Cluster I.

20, 40, 95, 200 or 300 ft below the surface. The final configuration of microphone was simply a hydrophone placed on the bottom of a 4 ft diameter plastic Kiddy Pool. The colorful Kiddy Pool served not only as the floating holder for the microphone but also as an easily identifiable reference position by which to guide the helicopter. The modified sonobuoy consisted of hydrophone, pre-amplifier, audio amplifier and transformer powered by a salt-water battery. Three sonobuoys were held together in a cluster. There were two clusters as shown in Fig. 4, one 300 ft from FLIP, the other either adjacent to or separated from the first by an additional in line, 150 ft. The microphone and hydrophones were hard-wired to a tape recorder in the instrument room on FLIP. The electrical cable was floated on one inch polypropylene line. Additional details of the mechanical, electrical and acoustical design and tests will be found in Ref. 11.

The signal from the sonobuoys was FM recorded on an 8 channel PI 6208 magnetic tape recorder, on board FLIP. One channel was reserved for voice annotation.

The data recorded during FLIPEX II consisted of calibrated, time-varying, voltages from hydrophones at 5 depths and a surface microphone during helicopter hovers at heights 40, 600 and 750 ft and 5 knot flybys and fly-overs at 150, 300, 600 and 750 ft.

Under the direction of Dr. Russ Davis of Scripps, time series wave height variations were recorded during both FLIPEX I and FLIPEX II. Whenever possible, such data were taken simultaneously with helicopter noise data. During FLIPEX II, four wave probes were used. Surface wave frequency spectra were generated by transforming the wave height variation time records for each device. Then mean square wave heights for several wave period ranges were obtained by integration of the

frequency spectra over appropriate frequency ranges. This processing was carried out at Scripps.

B. Data Analysis

1. Analogue Analysis

The frequency range 100 Hz to 1000 Hz corresponded to an acoustical roughness range, R, of approximately 0.05 to 4.0 for normally incident sound and for the typica l sea surface encountered during the experiment. Sixteen frequencies in this frequency range were selected for investigating the effect of a broad range of surface roughness on transmission and for comparison with theory.

The analysis utilized a Hewlett Packard Model 3590A wave analyzer with a General Radio Type 1163A frequency synthesizer used as an external local oscillator for the wave analyzer. The logarithmic output of the wave analyzer was used as the vertical input to a Varian Model F-100 X-Y recorder. This arrangement was particularly useful for analyzing and displaying the helicopter passes since the resulting plot showed the ambient noise levels before and after each pass as well as the total noise during each pass. A series of plots made for several frequencies using a typical helicopter pass appears in Fig. 5. The large time variation in rms level even with the slow response time of the wave analyzer is evident. Signal voltage levels for the helicopter passes were determined by taking an eyeball average of the time variations across the peak of the pass.

Ambient noise voltage levels between passes were determined in the same way. Since the plots represented rms levels in dB, this eyeball average of dB levels was something less than the true average rms voltage level. The error here was on the order of 0.5 dB. Since the type of time variation was about the same for the surface microphone as it was

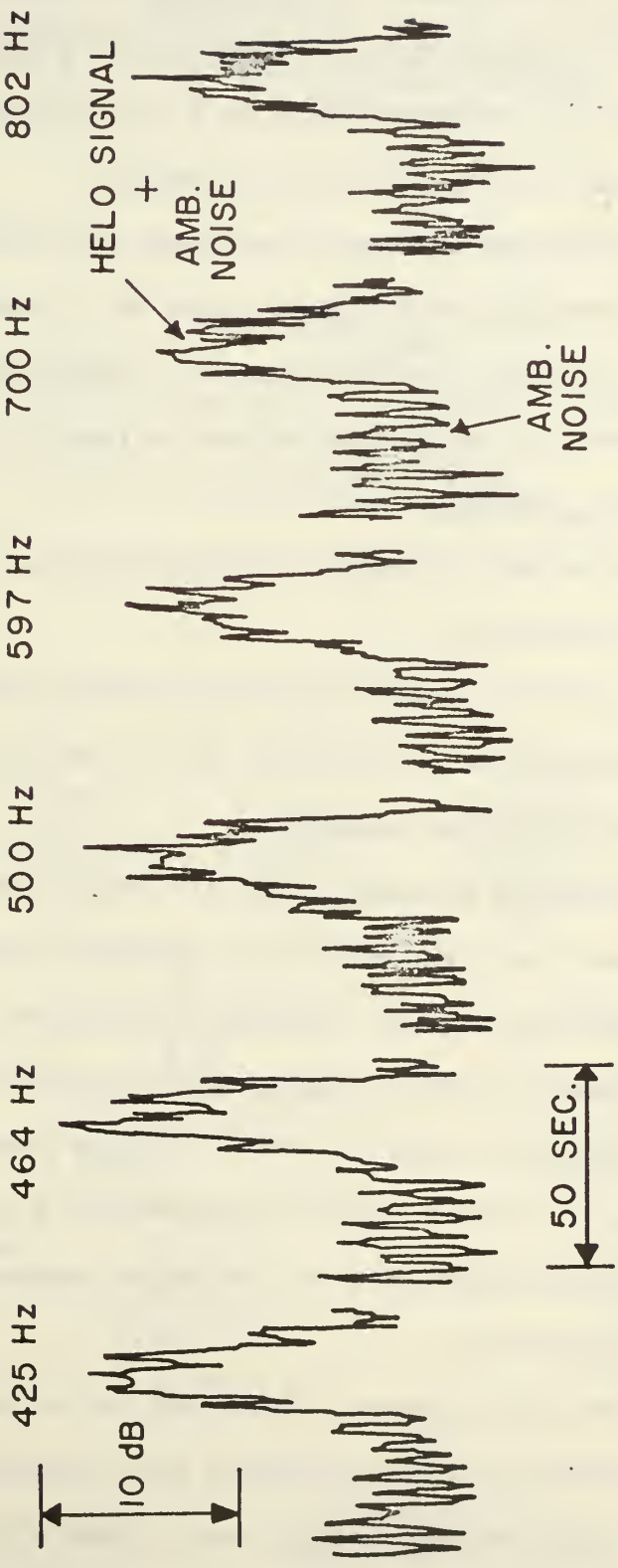

Figure 5. Strip chart records of sixty second samples of noise received in six 10 Hz bands as helicopter passed over the 40 ft deep hydrophone.

for the submerged hydrophones, this error canceled itself out when taking the difference to compute transmission change. To obtain helicopter signal voltage levels, the ambient noise voltage levels were subtracted off by using the white noise assumption. Signal sound pressure levels at the hydrophone were then determined by using the calibrated sensitivities of the transducers.

The Kirchhoff assumption was made in order to convert from observed microphone SPL to incident sound SPL. That is, it was assumed that pressure doubling had taken place so that the incident SPL was obtained by subtracting 6 dB from the surface SPL.

2. Digital Analysis

The major data reduction program for the transmission study was performed digitally.

Figure 6 is a general self-explanatory flow chart of the analysis. In addition to the flow chart, the following statements will help to characterize the analysis:

The sampling frequency was 2000/sec. Four channels, three hydrophones and one microphone, were sampled simultaneously. For each flyby or flyover experiment, data were digitized for peak sound levels when the helicopter flew directly over the mic and/or hydrophones. Additional data were taken in order to study changing sound levels within a time span which began approximately 50 sec before the helo approached the overhead position and ended approximately 50 secs after the overhead position.

Ambient noise levels, digitized for corresponding hydrophone depths, were taken at least one half hour preceding or succeeding each experiment. Most ambient signals were taken within minutes of an experiment and spanned a time period of approximately 15 seconds.

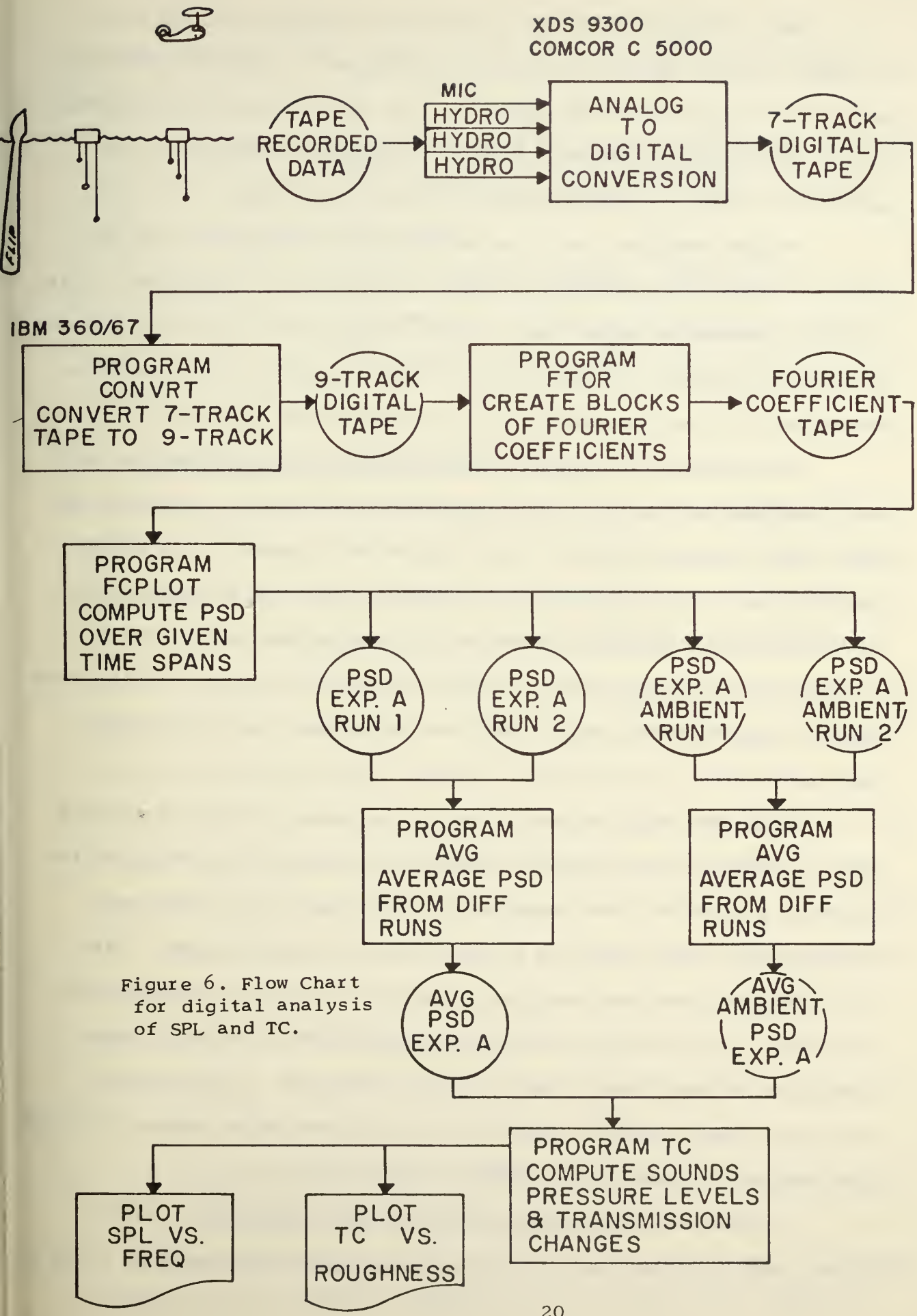

Figure 6. Flow Chart for digital analysis of SPL and TC.

After proper formatting of the tape, processing of the data was begun using a system of time series programs[12] originally developed by the University of British Columbia. The first program in the series, program FTOR, employs the FAST FOURIER TRANSFORM to compute Fourier coefficients from selected channels of the digital tape.

Program FTOR was run using varying block lengths of data in order to arrive at an adequate frequency resolution or bandwidth. After some experimentation using block lengths ranging from 2 secs to 1/8 sec, the decision was made to use blocks of 1024 samples (a duration of approximately 1/2 sec), giving a frequency resolution of 1.95 Hz.

Contiguous blocks of 2^{10} data points were transformed for each experiment and written on a "Fourier Coefficient Tape". This tape was then read by program FCPLOT of the time series programs. The FCPLOT program provides the capability of averaging over only selected blocks, e.g., over blocks spanning 10 second periods, or over all blocks as was the case for ambient data . This program was revised to write power spectral densities for given time spans on magnetic tape for further analyses.

From this tape of power spectral densities created by program FCPLOT, blocks of data corresponding in time were further averaged for different runs of a given experiment. For example, peak data were averaged for several runs and several ambients were averaged. Data from different runs were weighted according to the time span they represented. The averaged power spectral densities, along with their associated ambient levels, were read by program TC, a program which calculates sound pressure levels and sound transmission change and plots them against frequency and roughness, respectively.

Ambient noise was subtracted from helo-plus-ambient levels. Points were labelled "bad" if (helo-plus-ambient)-(ambient)$\leq$ 0, or if any

SPL differed by 20 dB or more compared to the SPL at a contiguous frequency.

An average TC was calculated for every 9 contiguous frequencies (band of 9.75 Hz). This average was considered "good" if 5 points out of the 9 were considered "good".

Because of many "bad" points caused by high ambient levels for $f < 100$ Hz, the "low frequency SPL" was calculated for the frequency band 100 to 200 Hz; the "overall SPL" was calculated for the frequency band 100 to 1000 Hz.

C. Comparisons of Experiments with Theory

During the course of the acoustical study, ocean height data were taken simultaneously at four probes, at a sample rate of eight times per second, The motions of FLIP were compensated for. The data for each probe were divided into four minute blocks, the spectra were computed, and then the spectra were averaged across these blocks. The wave height uncertainty for each of the runs is probably less than 5%. The wave height frequency spectrum for each probe was integrated to yield the mean squared height. The values of the mean squared height at the four probes were averaged and this average was used for the theoretical calculation of sound transmission changes. A calculation such as described was carried out for the ocean wave system twice on 17 August and twice on 18 August to yield values of rms heights, σ: 15.5 cm, 14.9 cm, 13.6 cm and 14.5 cm.

The general comparison with theoretical predictions is comprised of several single parametrical checks:

1. Variation of Transmission with Depth/Height Ratio for Normal Incidence at a Very Smooth Surface $R << 1$

When the surface is relatively smooth, $R << 1$, Eq. [20] tells us that only the coherent component of the transmission change is

significant. Further, if the surface is very smooth, $R \ll 1$, TC approaches TC_M (Eq. 14a) and the transmission change will be due only to the geometry and the ρc mismatch. The test is accomplished for the ocean experiment by calculating the average experimental TC for the low frequency band 100-200 Hz. For this band the surface acoustical roughness for normal incidence sound (fly-over or hover) was $R = 0.15$ at 200 Hz and one-quarter that value at 100 Hz. The decrease in coherent transmitted signal due to surface roughness, which goes as e^{-R}, would therefore be expected to be at most 0.68 dB at the high frequency end of the band and 0.16 dB at the low frequency end (100 Hz). This average expected loss of approximately 0.4 dB would not be distinguishable in this experiment. On the basis of the above argument, all observations of transmission change for the low frequency band, 100-200 Hz, are identified as occurring for $R \ll 1$ and are assumed to be equivalent to the values that would have been obtained for a mirror-like surface.

Figure 7 shows the transmission change at normal incidence predicted by mirror surface theory ($R \ll 1$) compared with experimental data taken in hovers and flyovers, at a height of 600 ft, for a decade of ratios of hydrophone depth, D, to source height, H. Only the low frequency band of sound frequencies have been used for this test. A positive value of TC represents an SPL at the hydrophone that is greater than the incident SPL at the surface. The average disagreement is approximately 2 dB. This small discrepancy could have been due to one or more of the following: the helicopter was not a proper point source: there was a difference in the absolute calibration of microphone and hydrophones; the pressure was somewhat <u>less</u> than doubled at the slightly rough surface.

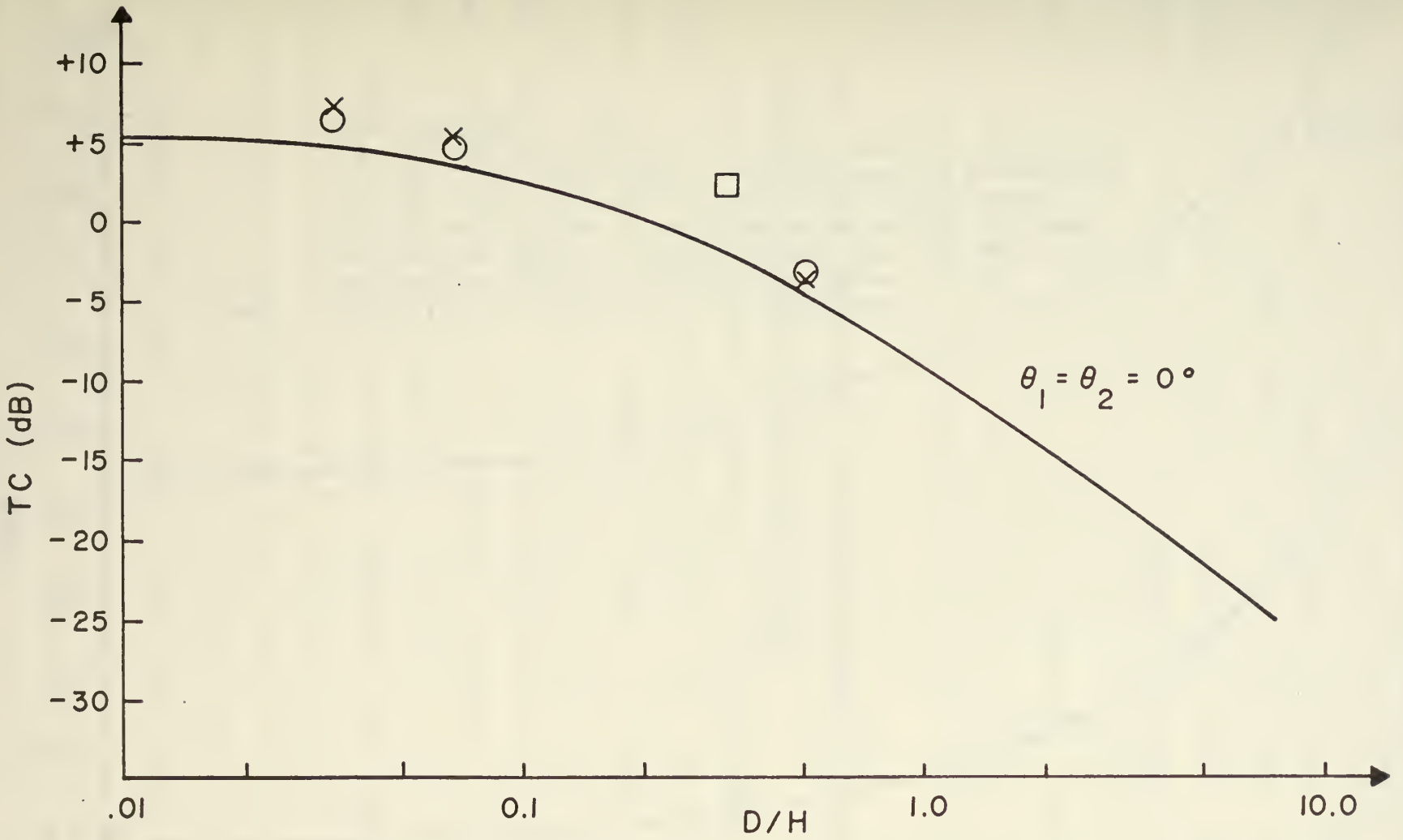

Figure 7. Transmission change, TC, as a function of depth to height ratio, D/H, for sound propagating at normal incidence, through an ocean surface of very small acoustical roughness, $R << 1$. Solid line is theoretical prediction, circles ○ are experimental values for a hovering helicopter, crosses, x, and squares □ are values obtained during fly-overs.

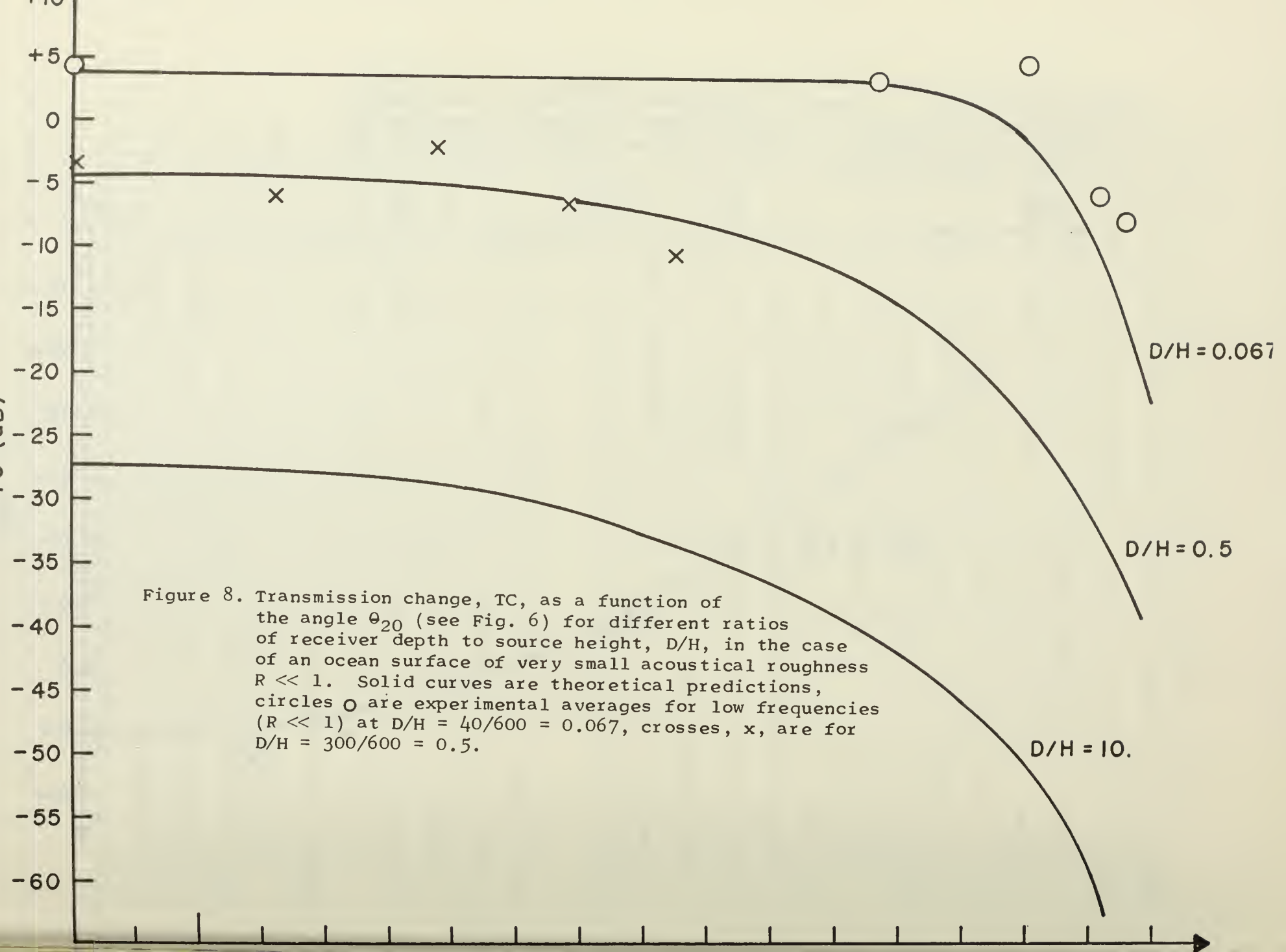

Figure 8. Transmission change, TC, as a function of the angle θ_{20} (see Fig. 6) for different ratios of receiver depth to source height, D/H, in the case of an ocean surface of very small acoustical roughness $R \ll 1$. Solid curves are theoretical predictions, circles o are experimental averages for low frequencies ($R \ll 1$) at D/H = 40/600 = 0.067, crosses, x, are for D/H = 300/600 = 0.5.

2. Variation of Transmission with Angle of Incidence at a Very Smooth Surface ($R \ll 1$) for a Constant Depth/Height Ratio

Figure 8 presents low frequency data taken during fly-overs. Each datum point represents average over eight or 16 blocks (each block is ½ second long) for cases in which the aircraft was either approaching (at 5 knots) or receeding. The geometry and the definition of θ_{20} are shown in Fig. 3. The assumption has been made (as above) that low frequency data for which ($R \ll 1$) should be compared with theoretical curves for the mirror surface TC_M. The comparison is again favorable for the two D/H ratios, 0.067 and 0.5, for which data were available. The theoretical curve for D/H = 10, is drawn for interest.

3. Variation of Transmission with Sound Frequency and Surface Acoustical Roughness; Source over Receiver

As the sound frequency increases, Eq. [20] predicts that the coherent term will dominate briefly and then for $R > 1$ the incoherent term will control the total transmission change. In order to calculate the expected transmission, Eq. [20] requires knowledge of the surface height correlation length L. This can be estimated from the known wind speed, by using the results of Cox and Munk to calculate first the rms slope[6] and then using the assumption of a Gaussian Correlation Length, L, to calculate its value; this simple calculation yields the approximate correlation length, $L \simeq 150$ cm for the ocean during FLIPEX II.

A second decision must be made before Eq. [20] can be used in the case of a point source; one must settle on the appropriate sub-areas ΔA_i. In principle they should be chosen so that the incident sound wave has uniform phase and amplitude over the subareas, and the correlation has dropped to effectively zero at the boundary of the subarea. Figure 9 shows the result of a computer study of the effect

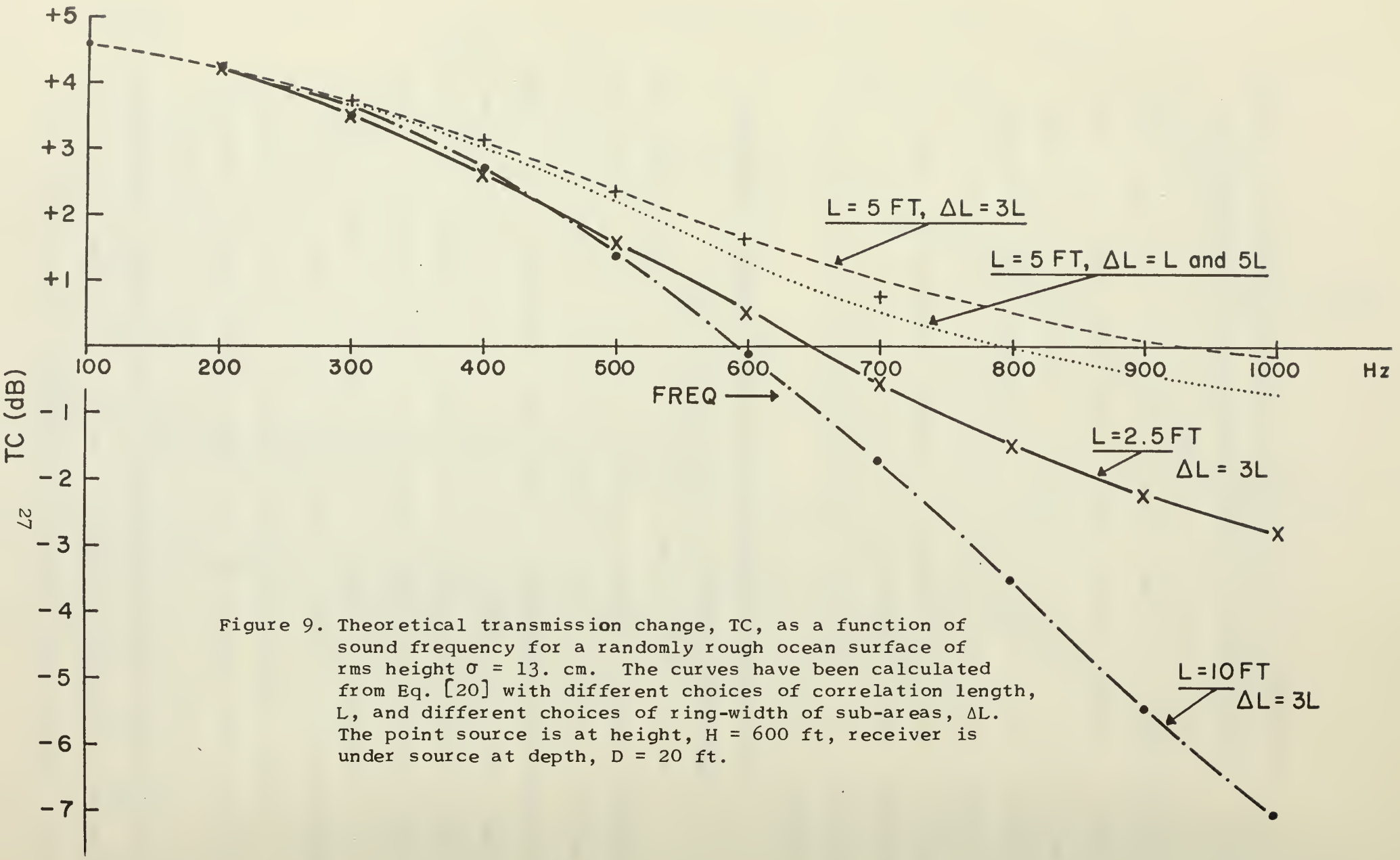

Figure 9. Theoretical transmission change, TC, as a function of sound frequency for a randomly rough ocean surface of rms height σ = 13. cm. The curves have been calculated from Eq. [20] with different choices of correlation length, L, and different choices of ring-width of sub-areas, ΔL. The point source is at height, H = 600 ft, receiver is under source at depth, D = 20 ft.

of a) changing the correlation lengths, L, and b) changing the width of the circular rings ΔL which define the sub-area. The calculation is for a source at 600 ft and a receiver at 20 ft for a sea of rms height, σ = 13. cm and correlation length, L $\simeq$ 150. cm (= 5 ft). It is observed that only the higher frequencies ($R > 1$) are controlled by these changes (that is, only the incoherent component is modified). Changing the correlation length from L = 2.5 ft to 5 ft to 10 ft with $\Delta L = 3L$ has the major effect on the transmission; changing the size of the sub-area rings from $\Delta L = L$ to $\Delta L = 3L$ or $\Delta L = 5L$, for the appropriate L = 5 ft has a smaller effect on the predicted transmission change, TC. Theoretical calculations of TC to be presented, below, were based on L = 5 ft and $\Delta L = 5L$ which fulfills assumption (2) of Section I-E.

It is not possible to simultaneously fulfill assumptions (1) and (3) of Section I-E for all the wave lengths studied in this experiment. Figure 10 presents the experimental data, analyzed by digital computer (solid line), and analogue playback, (circles). The two methods of analysis are in tolerable agreement. The low frequency experimental values of TC greater than +6 dB are clearly due to ambient noise underwater. The theoretical predictions (dashed line) appear to have approximately the correct dependence on roughness (or frequency squared). However theory appears to underestimate the amount of sound transmitted by roughly 5 dB for both the hydrophone at 20 ft depth and the one at 300 ft. Perhaps 2 to 3 dB of this discrepancy is the same as observed for $R \ll 1$ (Figure 7) and the explanation of section (1) could be repeated. However, it is probable also that the simple theory for adding sub-areas that was developed in reference 1 underestimates the contributions of the incoherent sound in the region $R \geq 1$.

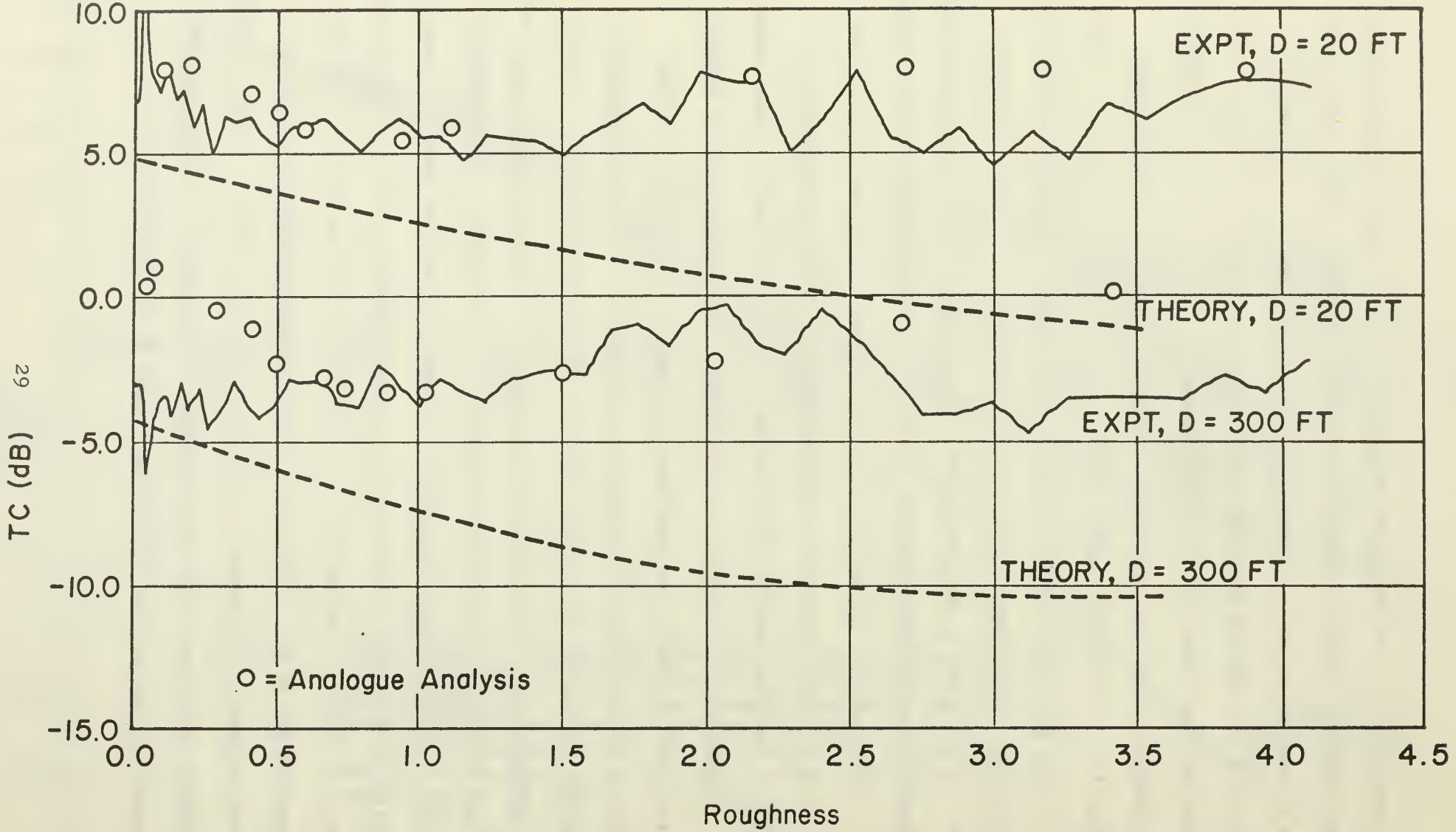

Figure 10. Transmission change as a function of surface acoustical roughness, R, for a point source at 600 ft above the sea, receivers at depth 20 and 300 ft under the source. Solid lines are results of digital analysis of the data, circles are analogue results. The dashed lines were calculated from Eq. [20] using measured sea conditions, rms height σ = 13. cm, correlation length L ≃ 150. cm.

The transmission change for normal incidence sound is seen to be only slightly dependent on acoustical roughness (frequency squared). For example the experimental curves could be crudely summarized as showing a constant TC $\pm$ 2 dB. It is this small spectral variation for near-overhead sources that has permitted some researchers to ignore the frequency dependence, completely, and to assume that the mirror value TC_M Eq. [14] as valid for all frequencies. This fortuitous situation is due, in fact, to large incoherent contributions from non-Snell directions which compensate for the decrease in transmission of the coherent component, as the frequency is increased.

The jaggedness in the experimental data is, of course, due to inadequate averaging time being available. Much of the data represent averaging over 10 to 20 seconds, whereas 10 to 20 minutes would be necessary to reduce adequately the statistical variations.

Additional experimental curves of transmission change for the helicopter over the hydrophone are given in Figures 11-25. Figures 11-13 represent hovers nominally over the hydrophones at 20, 40 and 300 ft respectively. In fact, the helicopter pilot had difficulty seeing the float marker and maintaining position during the hover at 600 ft altitude and unintentional off-sets of as much as 100 ft, may have been present. Our study of the playback gave evidence of the helicopter drift and permitted the extraction of the 24 second analysis presented in Figures 11-13 which we believe represents the true over-head position. The coherent, e^{-R}, dependence for $0.2 < R\ 0.5$ is fairly clear in these cases because of longer averaging time; the straight line starting at TC = 0 shows the predicted slope of an e^{-R} dependence. The data for $R < 0.2$ are unreliable because of strong and variable ambient noise levels. The hover analysis yields virtually the same TC data as the fly-over analysis shown in Figure 10.

Figures 14 and 15 represent 5 sec and 3 sec analyses for source at 600 ft over the hydrophone at 20 ft. The 150 ft offset of the source relative to the microphone would have a small effect on the incident levels; an inverse-square correction has been made for this. The two curves show the type of variation of TC that can take place due to a different sea surface at the time of analysis and due to an inadequate time of analysis. Some of the jaggedness is eliminated when the 8 sec average is taken; this average was presented in Figure 10. Figure 16 represents an 8 second average for the overhead source at 600 ft and receiver at 40 ft; it should be compared with the curves on Figure 10 from which it was omitted to avoid crowding.

Figure 17 shows the transmission change for a pass directly over Cluster II containing microphone and 95 ft hydrophone. It too can be compared with curves on Figures 10, from which it was excluded to avoid crowding.

4. Variation of Transmission with Sound Frequency and Surface Acoustical Roughness; Source Offset From Receiver

When the source is not directly over the receiving hydrophone, our theory again gives a fairly good prediction of experiment. Figure 18 shows the comparison of theory and experiment for an offset of approximately 250 ft, resulting in an angle from hydrophone, θ_{20} of 85° for the 20 ft receiver and 40° for the 300 ft deep receiver. In the case of the 20 ft hydrophone, simple mirror theory would predict a transmission loss of more than 15 dB for all frequencies. The theory of Eq. [20] comes closer to the mark because it accounts for the incoherent contributions which become important at $R > 1$.

The region $R < 0.5$ is of particular interest because of the so-called "evanescent", "inhomogeneous", or "lateral" wave that theorists[13-14] predict would be refracted through a smooth interface.

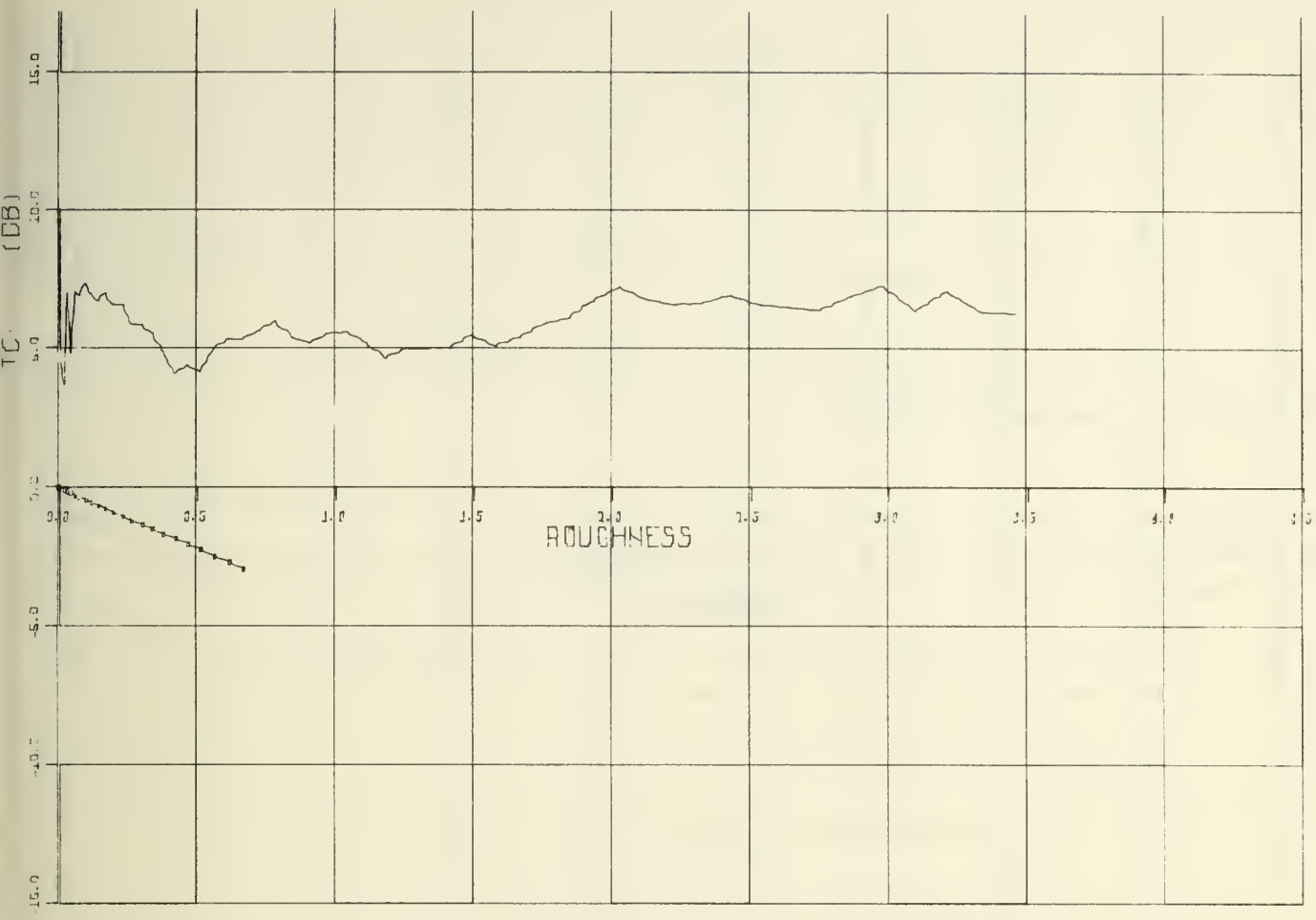

EXP. 11 - HOVER

HELO ALTITUDE = 600.0 FT. HYDROPHONE DEPTH = 20.0 FT.

HELO OFFSET FROM MIC FLOAT - VARIED

HELO OFFSET FROM HYDRO FLOAT - VARIED

THETA1 = 0.00 DEG. THETA2 = 0.00 DEG.

NO. OF BLKS = 48 (1/2 SEC BLKS)

Figure 11. Transmission change in SPL as a function of surface acoustical roughness for helicopter hover at 600 ft over hydrophone at 20 ft depth.

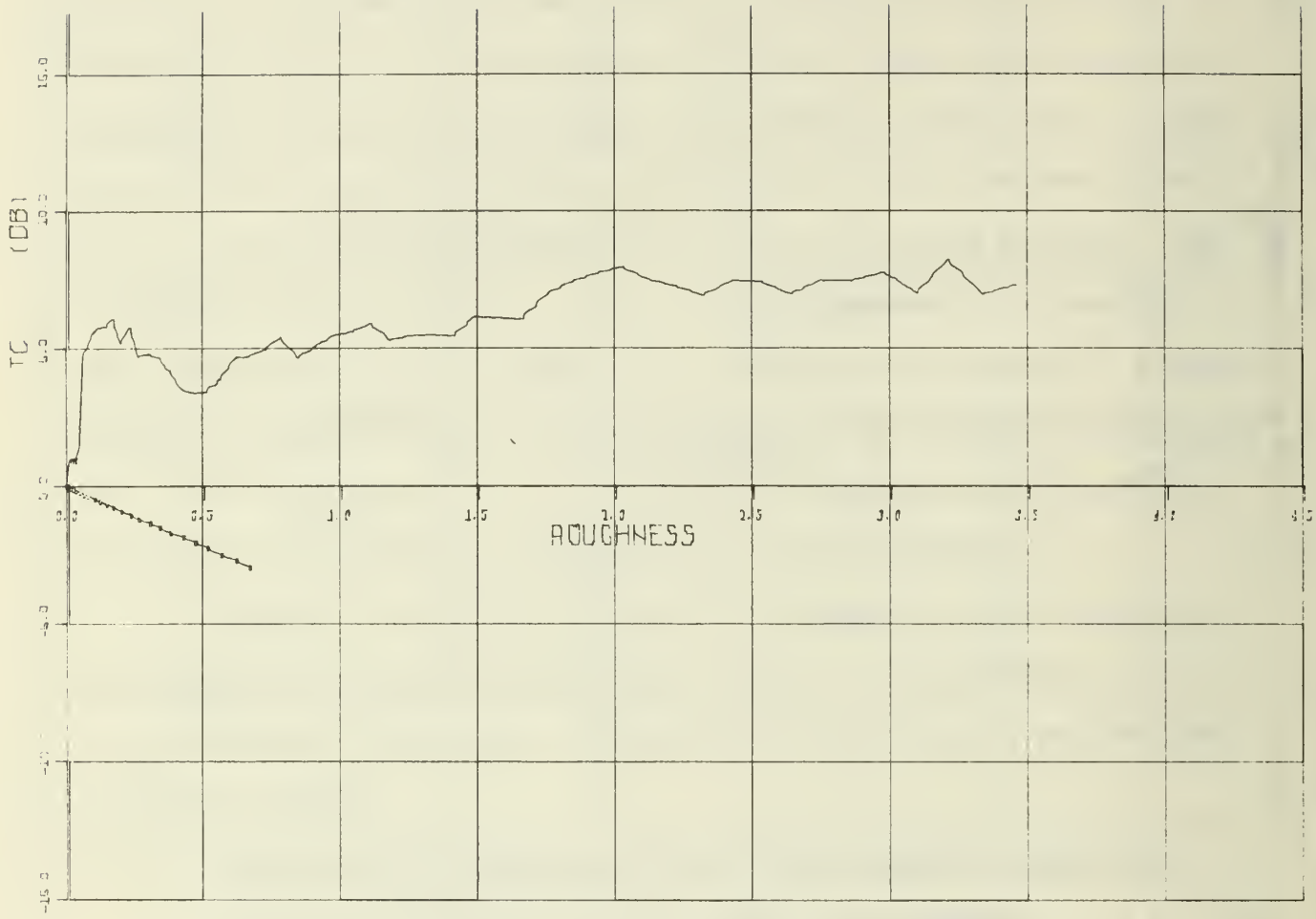

EXP. 11 - HOVER

HELO ALTITUDE = 600.0 FT. HYDROPHONE DEPTH = 40.0 FT.

HELO OFFSET FROM MIC FLOAT - VARIED

HELO OFFSET FROM HYDRO FLOAT - VARIED

THETA1 = 0.00 DEG. THETA2 = 0.00 DEG.

NO. OF BLKS = 40 (1/2 SEC BLKS)

Figure 12. Same as Figure 11 but with hydrophone at 40 ft depth.

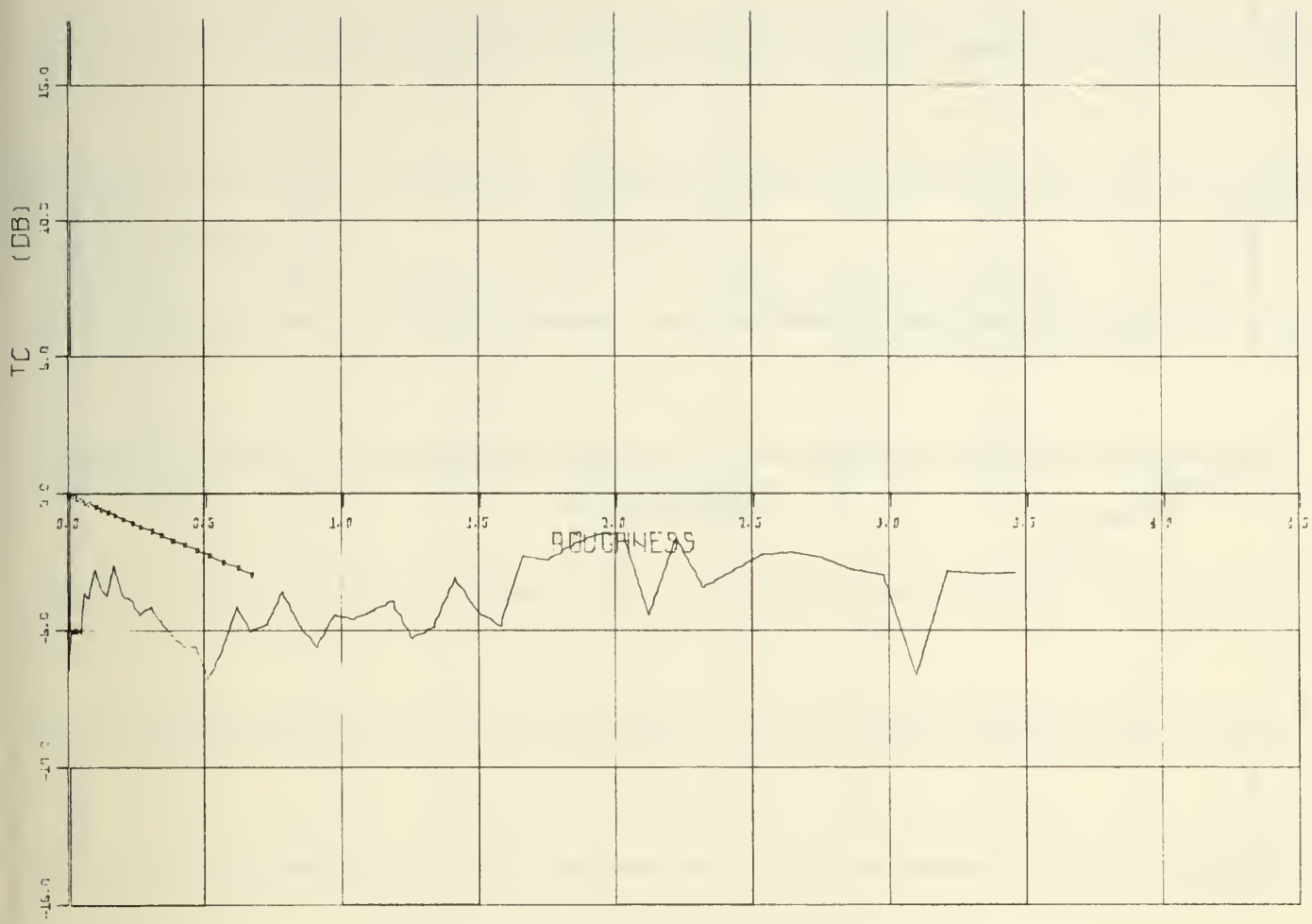

EXP. 11 - HOVER

HELO ALTITUDE = 600.0 FT. HYDROPHONE DEPTH = 300.0 FT.

HELO OFFSET FROM MIC FLOAT - VARIED

HELO OFFSET FROM HYDRO FLOAT - VARIED

THETA1 = 0.00 DEG. THETA2 = 0.00 DEG.

NO. OF BLKS = 48 (1/2 SEC BLKS)

Figure 13. Same as Figure 11 but with hydrophone at 300 ft depth.

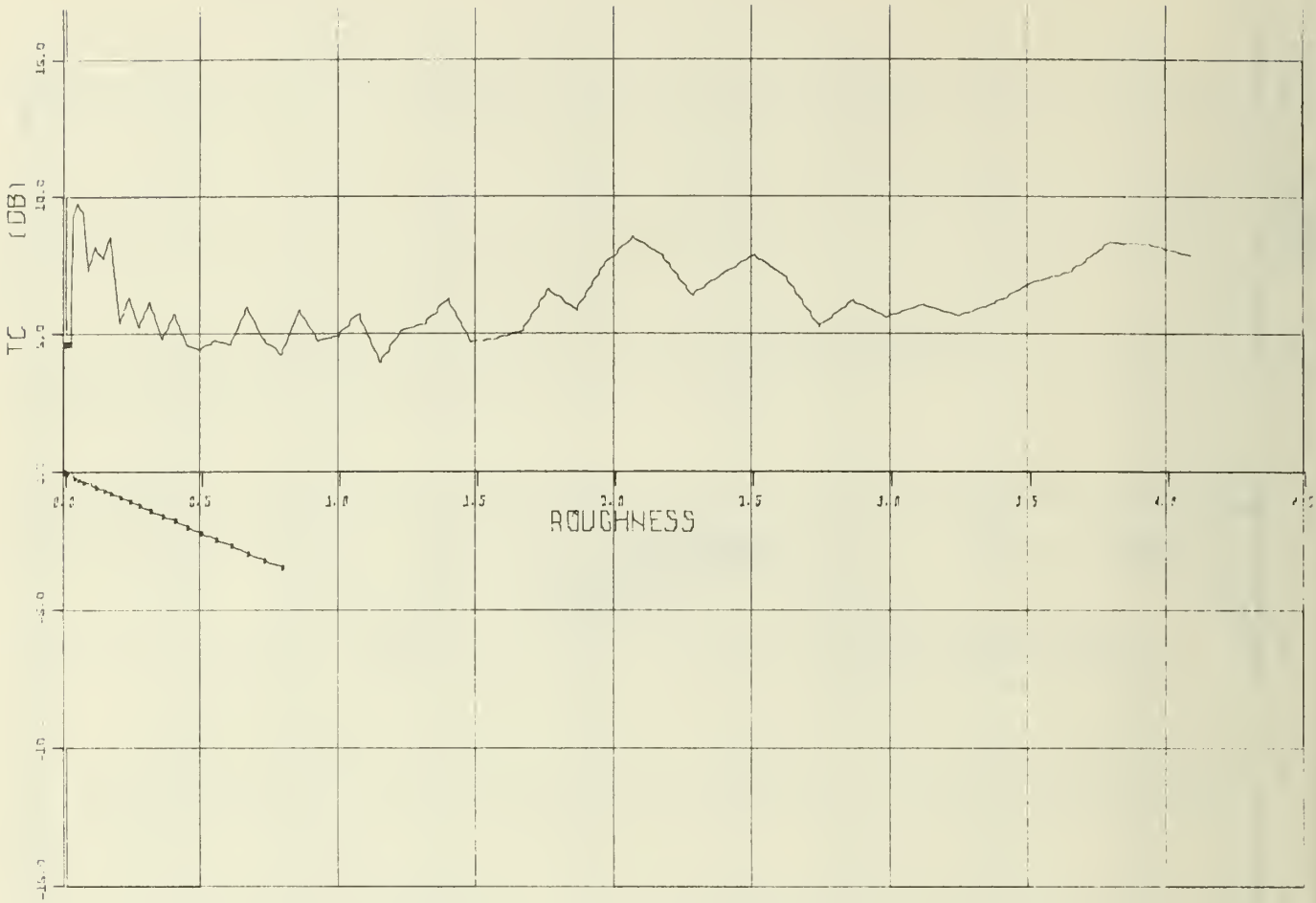

EXP. 17 - RUN 18 - FLYBY

HELO ALTITUDE = 600.0 FT. HYDROPHONE DEPTH = 20.0 FT.

HELO OFFSET FROM MIC FLOAT = 150 FT

HELO OFFSET FROM HYDRO(1) = 0 FT.

THETA1 = 0.00 DEG. THETA2 = 0.00 DEG.

NO. OF BLKS = 10 (1/2 SEC BLKS)

Figure 14. Transmission change as a function of surface acoustical roughness for a helicopter fly-by at 600 ft over hydrophone at 20 ft depth.

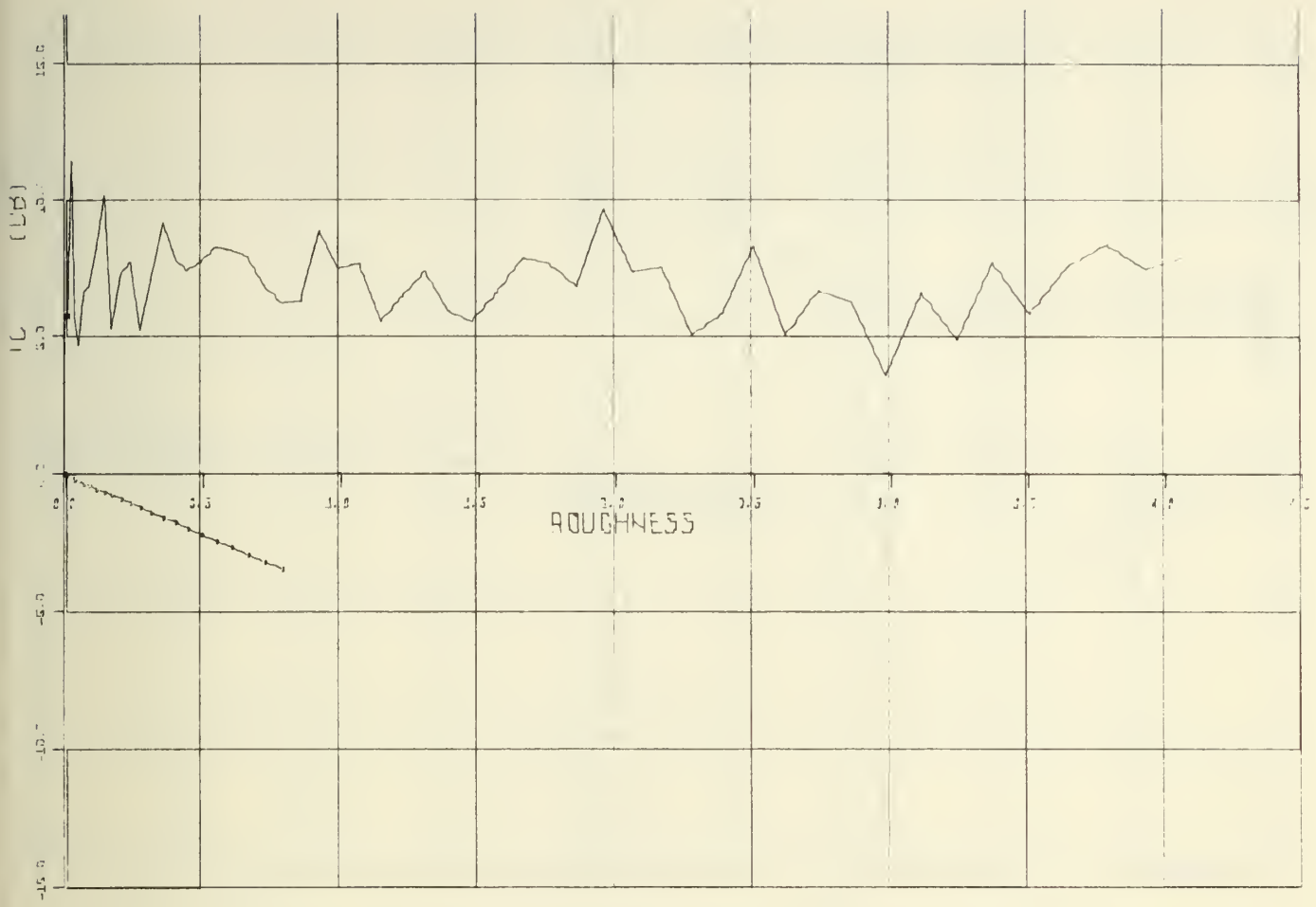

EXP. 17 - RUN 19 - FLYBY

HELO ALTITUDE = 600.0 FT. HYDROPHONE DEPTH = 20.0 FT.

HELO OFFSET FROM MIC FLOAT = 150 FT

HELO OFFSET FROM HYDRO(1) = 0 FT.

THETA1 = 0.00 DEG. THETA2 = 0.00 DEG.

NO. OF BLKS = 6 (1/2 SEC BLKS)

Figure 15. Same as Figure 14 but a different fly-by.

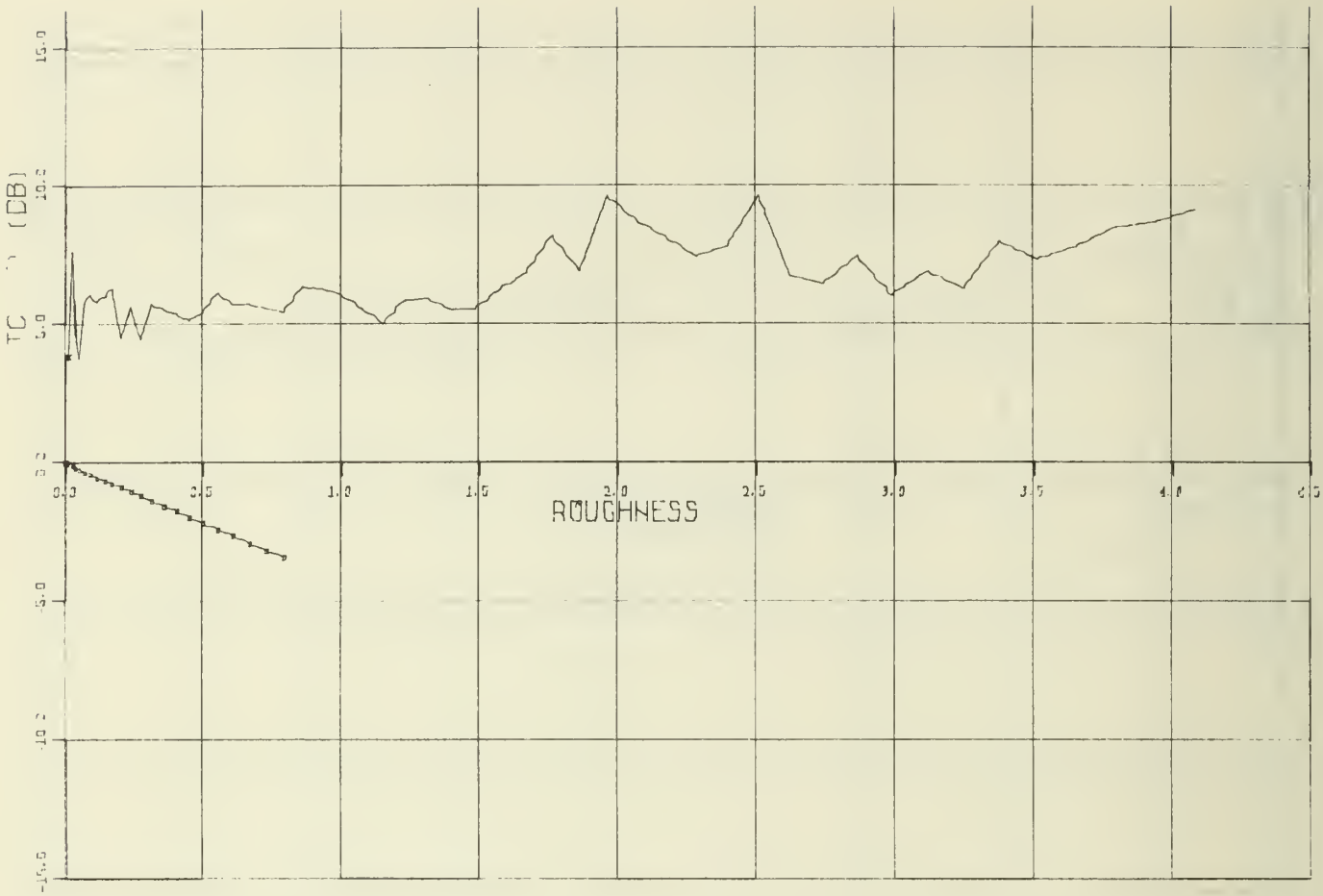

EXP. 17 - FLYBY - AVG. OVER 2 RUNS

HELO ALTITUDE = 600.0 FT. HYDROPHONE DEPTH = 40.0 FT.

HELO OFFSET FROM MIC FLOAT = 150 FT

HELO OFFSET FROM HYDRO(1) = 0 FT.

THETA1 = 0.00 DEG. THETA2 = 0.00 DEG.

NO. OF BLKS = 16 (1/2 SEC BLKS)

Figure 16. Average transmission change as a function of surface acoustical roughness for two helicopter fly-bys at 600 ft over hydrophone at 40 ft depth.

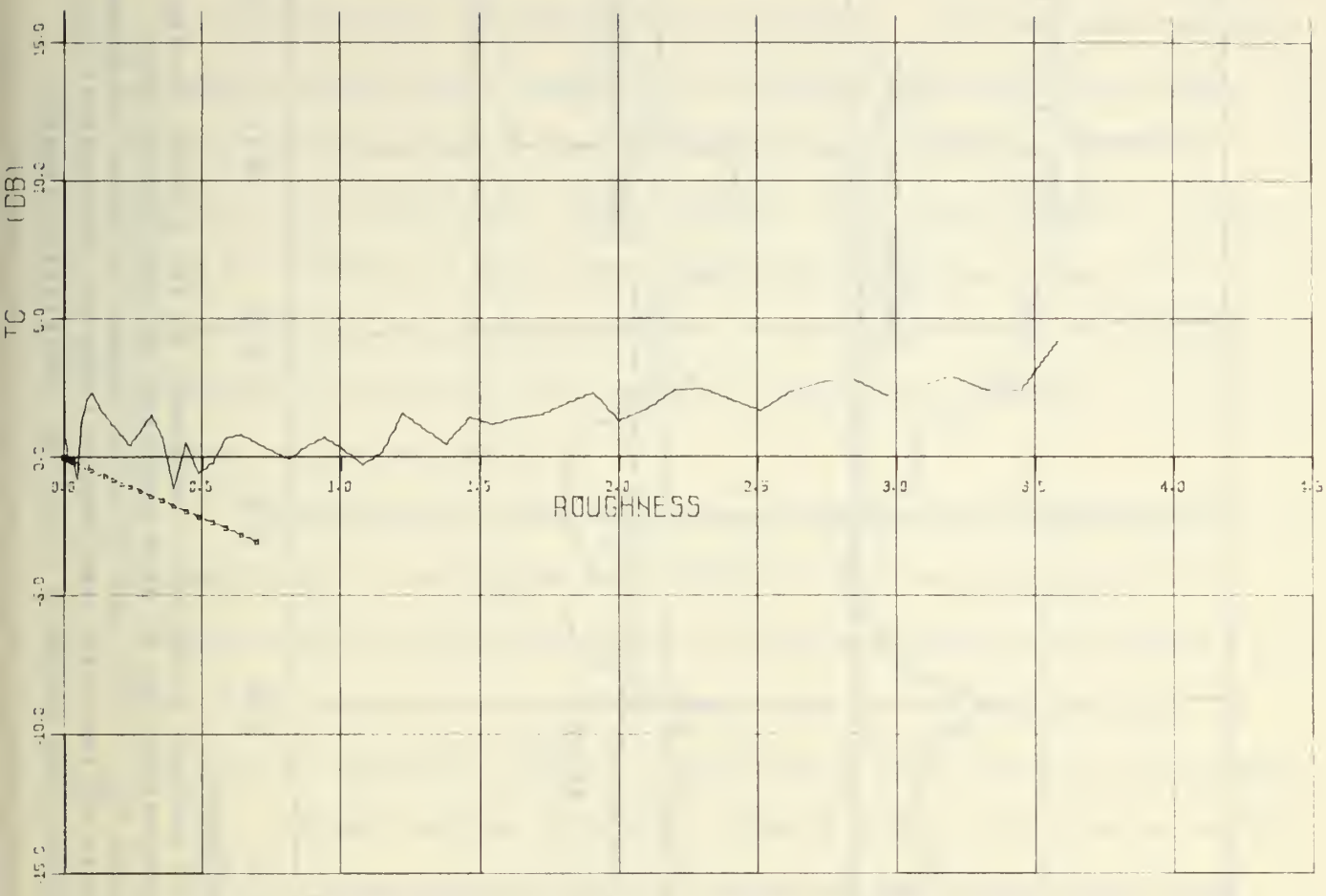

EXP. 13 - FLYOVER - PEAK PLUS 0 SECS

HELO ALTITUDE = 600.0 FT. HYDROPHONE DEPTH = 95.0 FT.

HELO OFFSET FROM MIC FLOAT = 0 FT.

HELO OFFSET FROM HYDRO(II) = 0 FT.

THETA1 = 0.00 DEG. THETA2 = 0.00 DEG.

NO. OF BLKS = 22 (1/2 SEC BLKS)

Figure 17. Transmission change as a function of surface acoustical roughness for a helicopter fly-by at 600 ft over hydrophone at 95 ft depth.

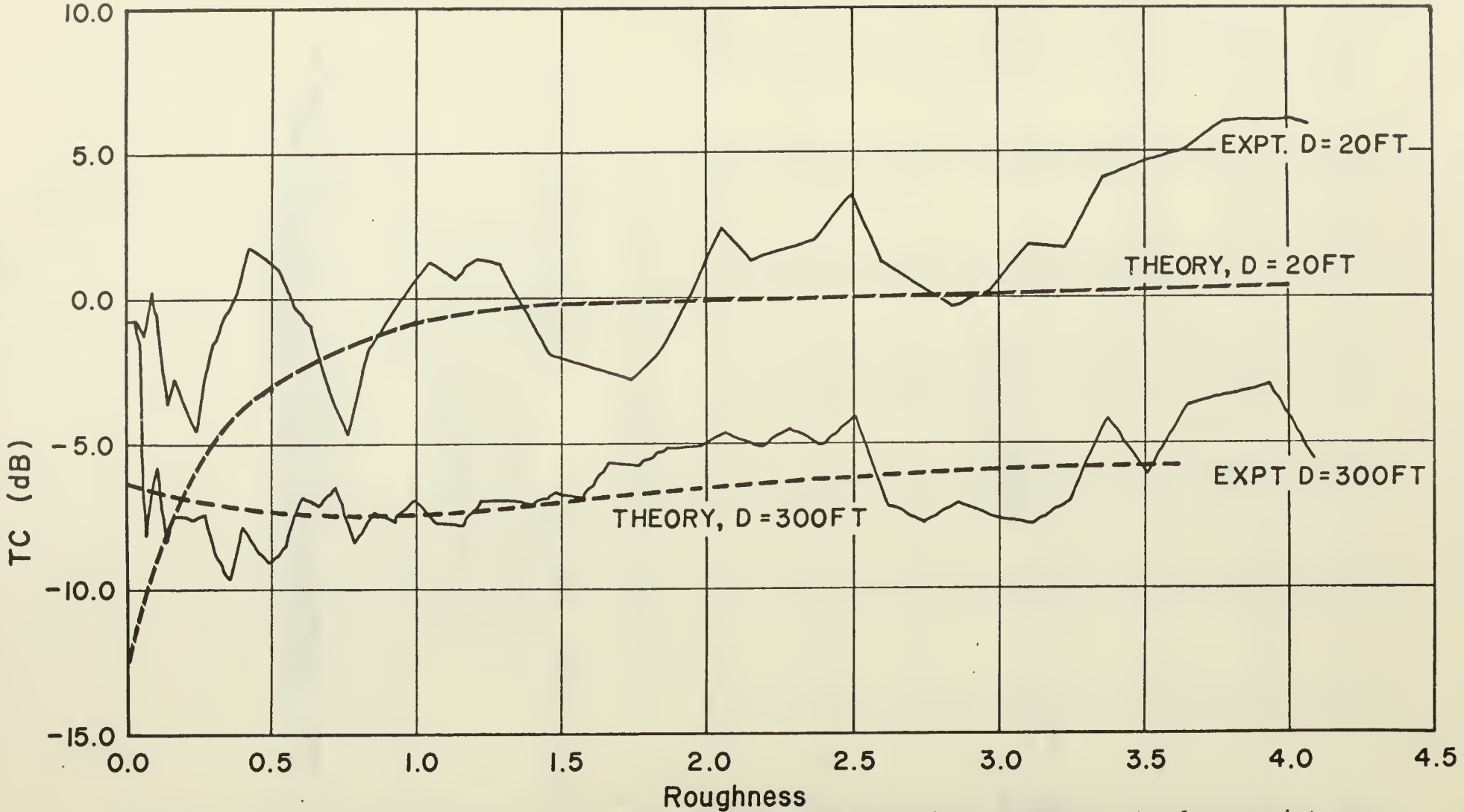

Figure 18. Transmission change as a function of surface acoustical roughness, R, for a point source 600 ft above the sea. Source is offset by approximately 250 ft from position of receivers so that hydrophones at 20' and 300 ft depth are at angles $\theta_{20} = 85^{o}$, and 40^{o} with respect to normal at ground zero. Solid lines are results of digital analysis of the data, the dashed lines are theoretical predictions of Eq. [20] using measured sea conditions, rms height σ = 13. cm, correlation length $L \simeq 150.$ cm.

Our theory has not considered this component. The fact that the low frequency sound levels underwater are higher than predicted by our theory (see also Fig. 8 with D/H 0.067) may be evidence that a laterial wave exists for rough surfaces, too; unfortunately, it may also be evidence of the strong low frequency ambient noise that was present during the experiment and/or refraction to the 300 ft hydrophone due to a strong ($9C^{o}$) negative temperature gradient that existed between 60 ft and 240 ft.

Figures 19-21 show transmission changes as a function of roughness for a helicopter pass directly over the microphone but offset by 150 ft from the string of three hydrophones of Cluster I at depths 20, 40, 300 ft. The helicopter was moving perpendicular to the line of Clusters I and II, when these offset data were collected.

The next series of graphs, Figures 22-25, show spectra of TC at various times during 5 knot fly-overs at 600 ft altitude, using hydrophones at depths 20, 40 and 300 ft. Now the helicopter moves perpendicular to the line of Clusters I and II so as to pass over the hydrophones. In Figure 22 we see three curves for the 20 ft hydrophone representing (from bottom to top): source 50 sec (410 ft) offset and approaching; source 30 secs (250 ft) offset and approaching; source overhead.

Figures 23 shows the spectra of TC for the receding helicopter as it continues to fly slowly along the path perpendicular to the line of the microphone-hydrophone clusters: passing over the 20 ft hydrophone in the top curve; 40 sec (330 ft) past the hydrophone cluster in the middle curve; and 50 sec (410 ft) past in the bottom curve.

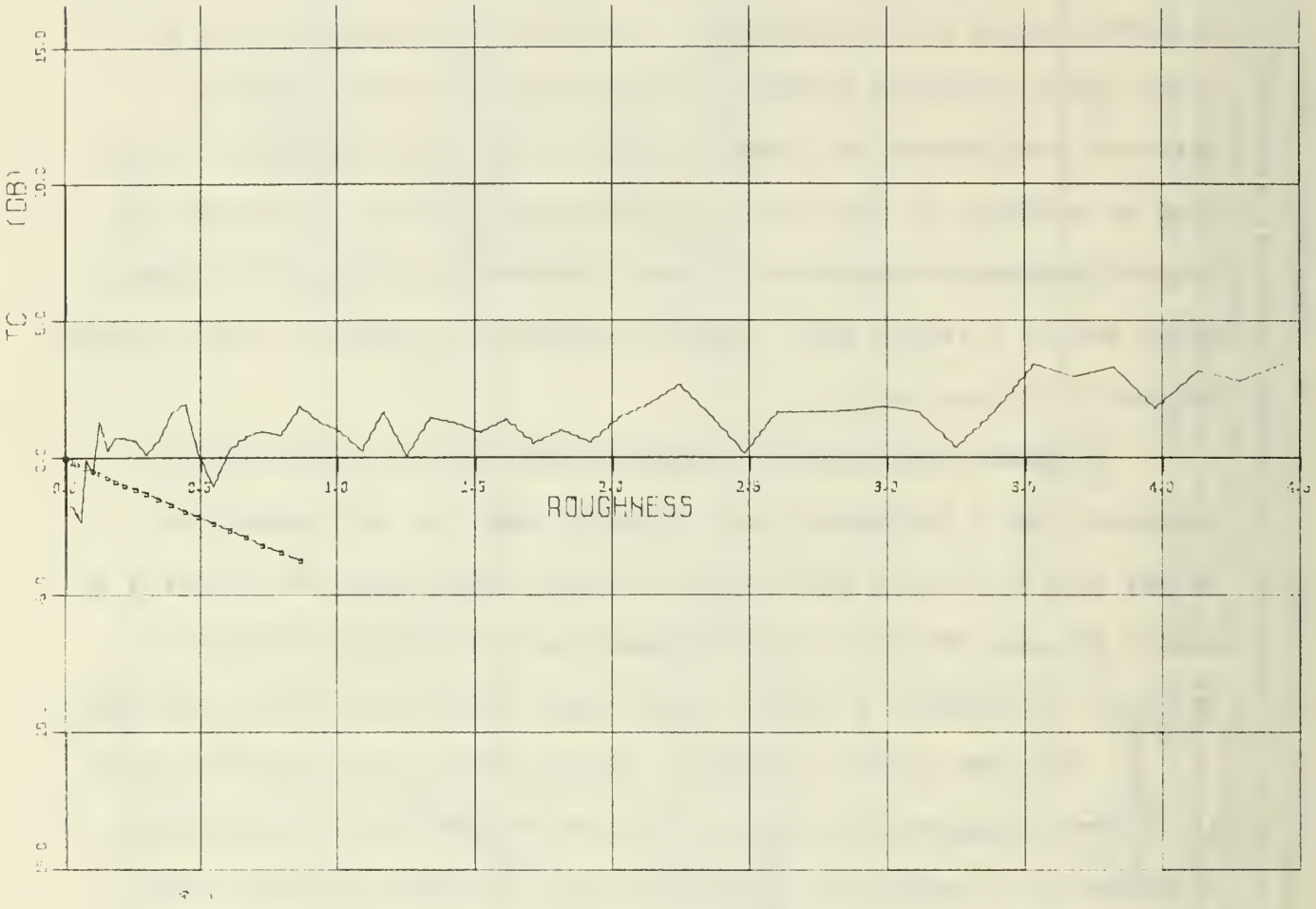

Figure 19. Transmission change as a function of surface acoustical roughness for helicopter offset by 150 ft from 20 ft deep hydrophone. See text for details.

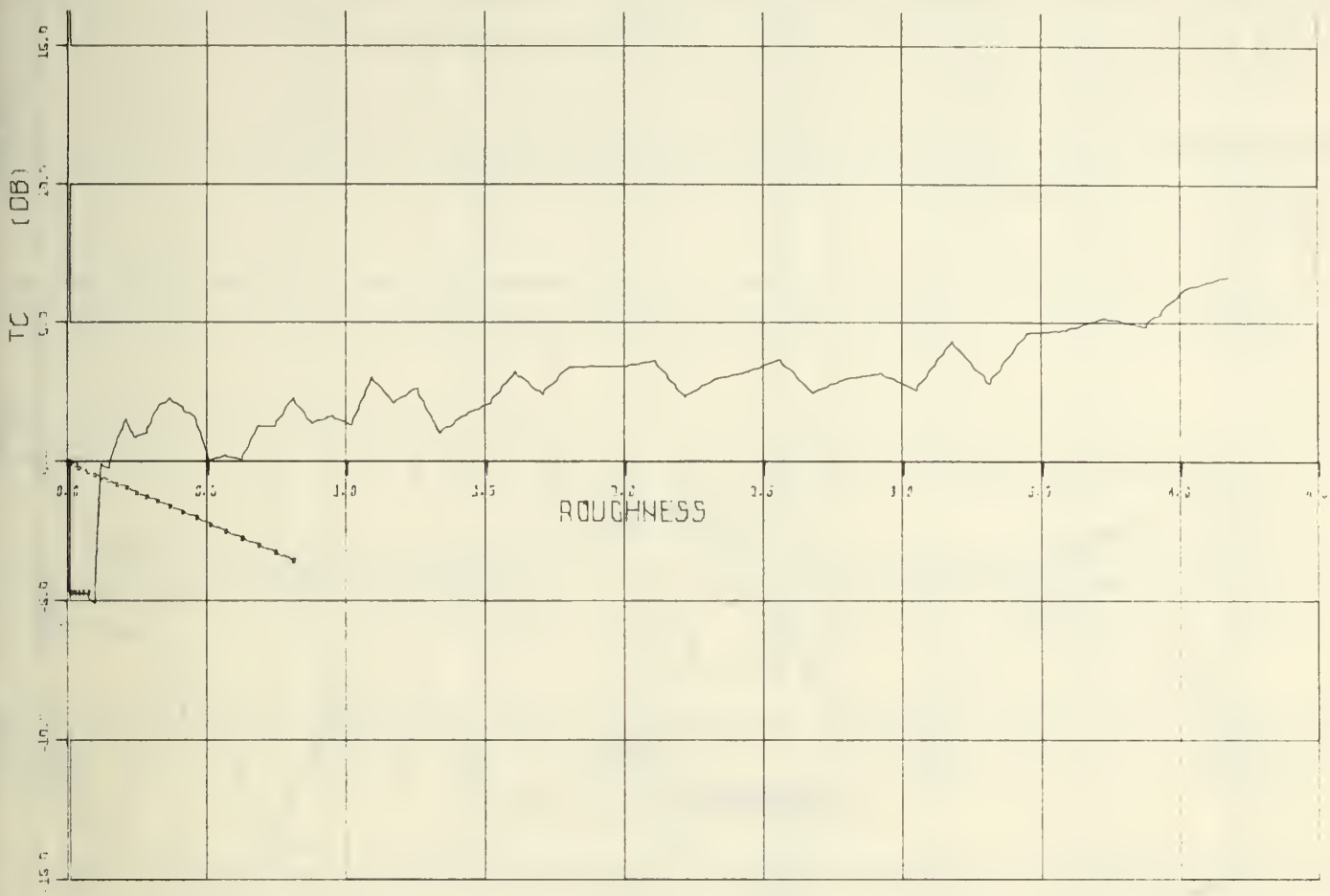

EXP. 13 - FLYOVER

HELO ALTITUDE = 600.0 FT. HYDROPHONE DEPTH = 40.0 FT.

HELO OFFSET FROM MIC FLOPT = 0 FT.

HELO OFFSET FROM HYDRO(1) = 150 FT.

THETA1 = 9.93 DEG. THETA2 = 48.37 DEG.

NO. OF BLKS = 23 (1/2 SEC BLKS)

Figure 20. Same as Figure 19 but with hydrophone at 40 ft depth. See text for details.

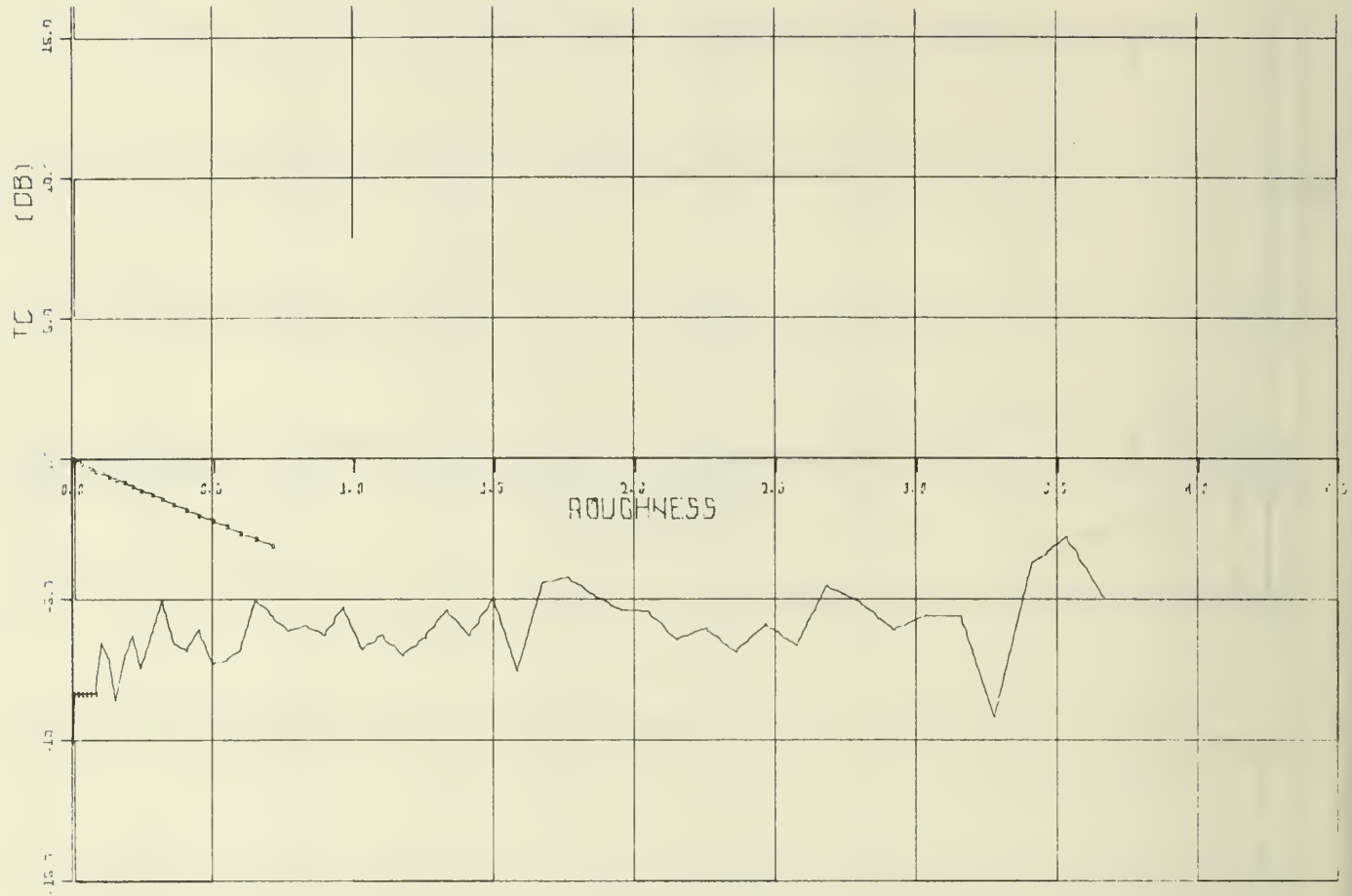

Figure 21. Same as Figure 19 but with hydrophone at 300 ft depth. See text for details.

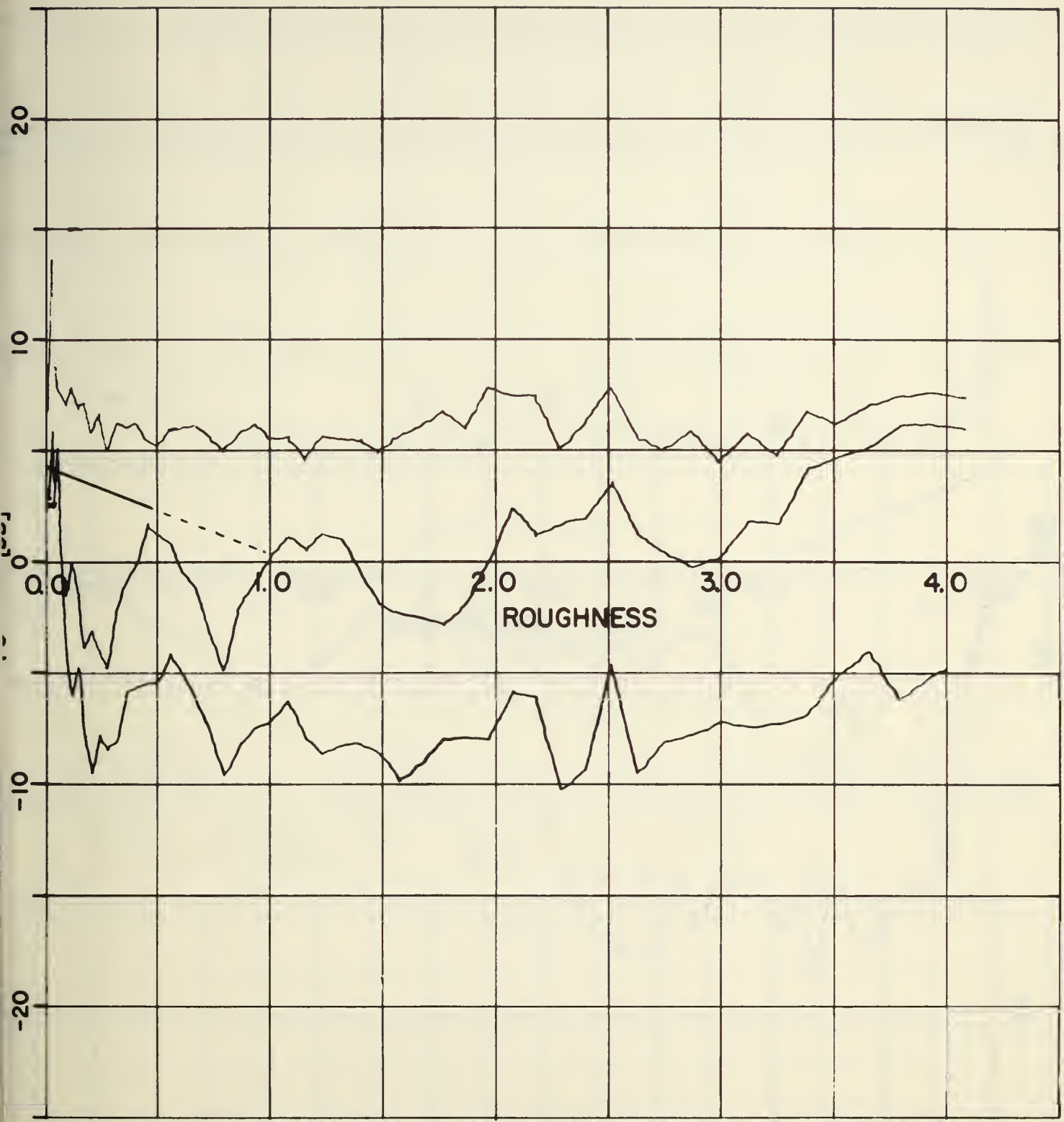

Figure 22. Transmission change as a function of surface acoustical roughness for H = 600 ft, D = 20 ft at different positions of flyby. See text for details.

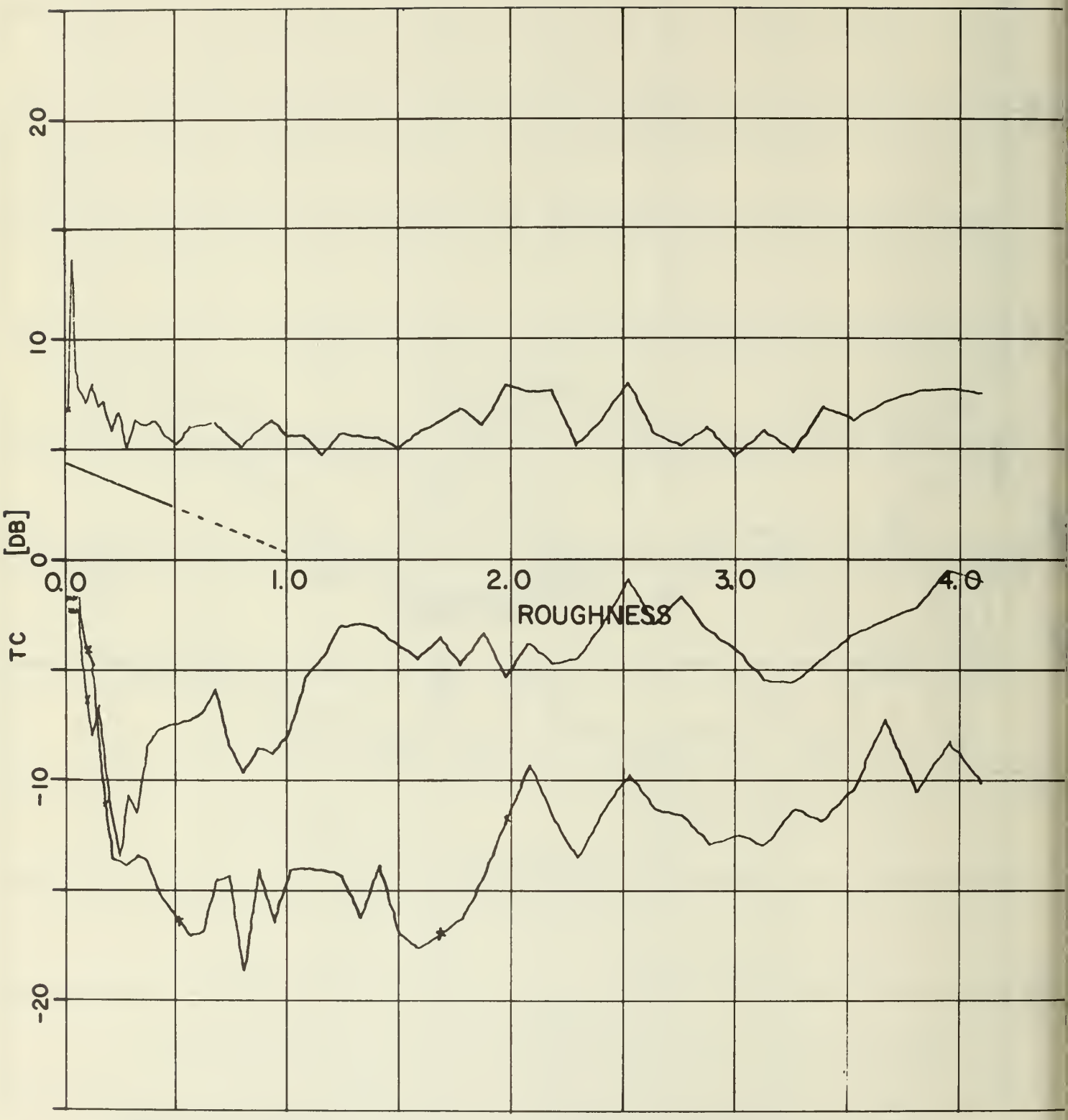

Figure 23. Same as Figure 22; see text for details.

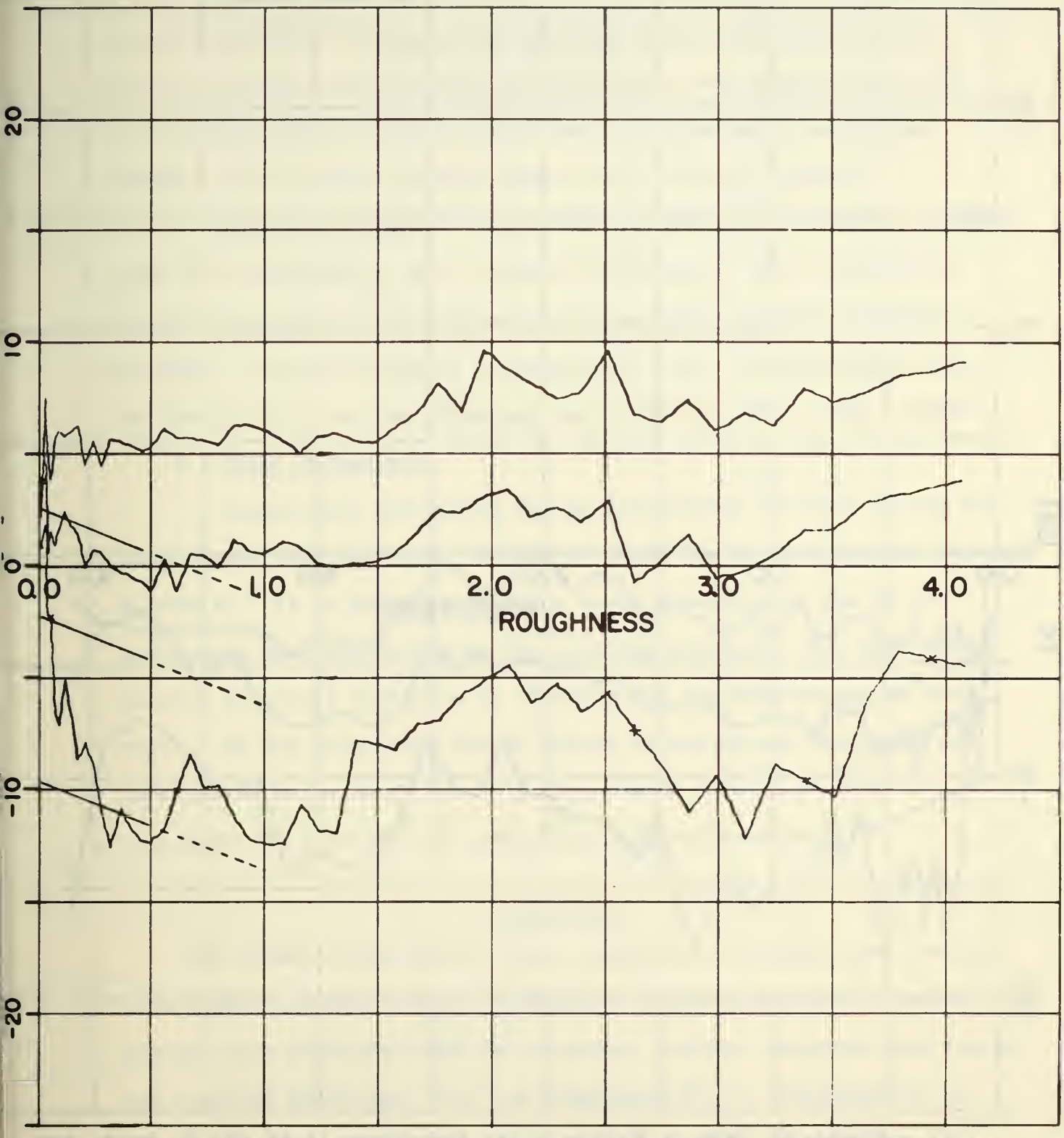

Figure 24. Same as Figure 22, but hydrophone is at 40 ft depth; see text for details.

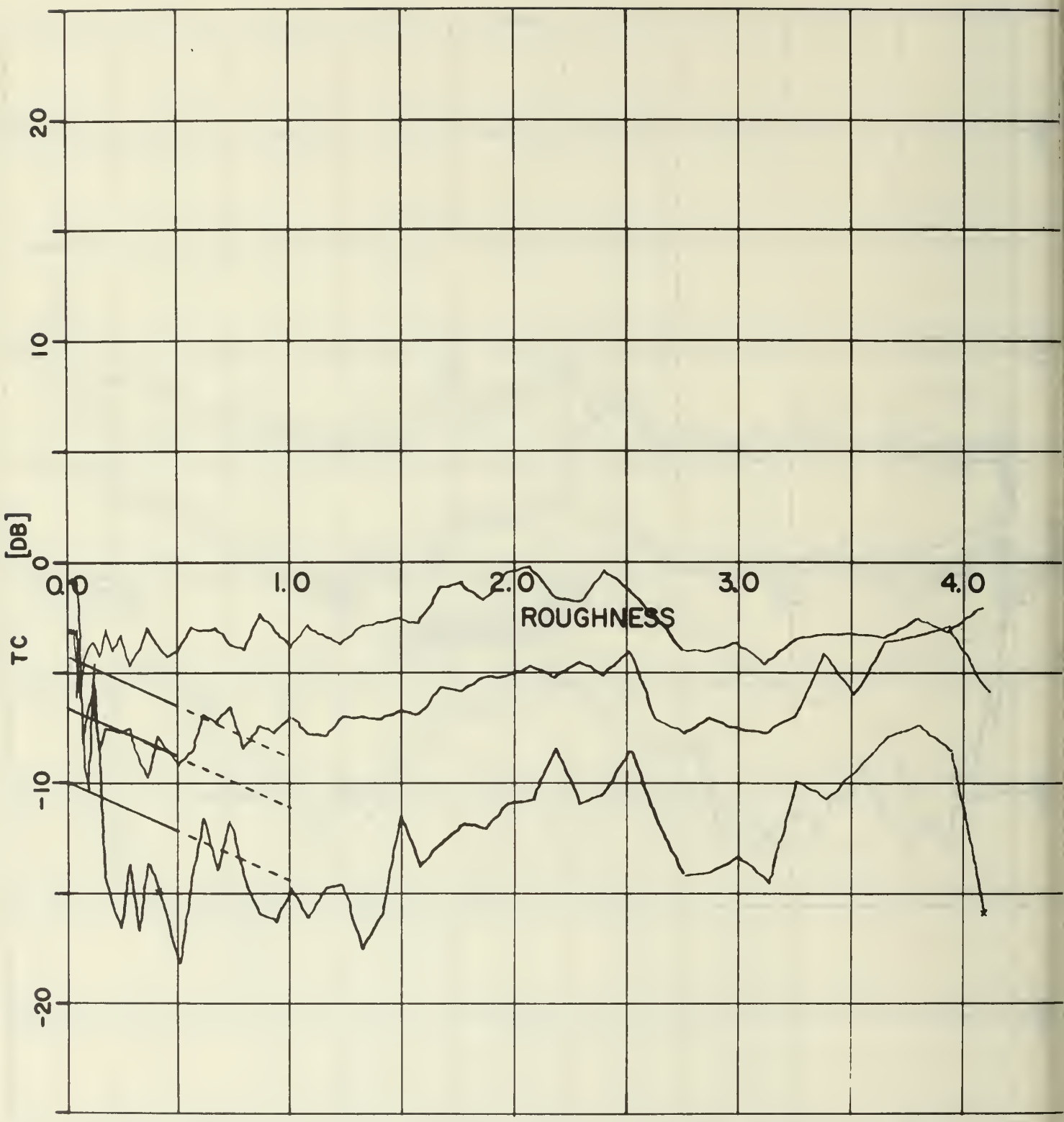

Figure 25. Same as Figure 22 but hydrophone is at 300 ft depth; see text for details.

Figure 24 shows TC under the same conditions as described in the previous figure except that hydrophone is 40 ft below surface. The top curve is for the overhead helicopter; the middle curve for the source receding and at 165 ft from overhead; the bottom curve for the source receding and at 250 ft from overhead.

Figure 25 presents TC for the same conditions of flyby except that the hydrophone is 300 ft below the surface. The top curve is for the helicopter overhead position; the middle curve is for the receding helicopter now at a distance of 250 ft from overhead; the bottom curve is for the receding helicopter at 410 ft from overhead.

5. Other Parameters

Temperature refraction was an unavoidable variable during the experiments reported here. Figure 26 shows the BT plot typical during FLIPEX II. It is believed that the sound pressures at the 20 ft hydrophone were unaffected by the existing gradient. Nor would the results at normal incidence be affected for the hydrophones at any depth. On the other hand the TC curves at non-normal incidence for hydrophones below 20 ft are only approximate because we have not corrected the data for the temperature refraction effect.

III. CONCLUSIONS

The Helmholtz-Kirchhoff theory, applied to transmission from air into water, provides useful predictions of the dependence of transmitted sound pressure level on frequency, surface roughness and source and receiver positions. For low roughness, $R < 1$, transmission is essentially the same as for a smooth surface, but decreased by the

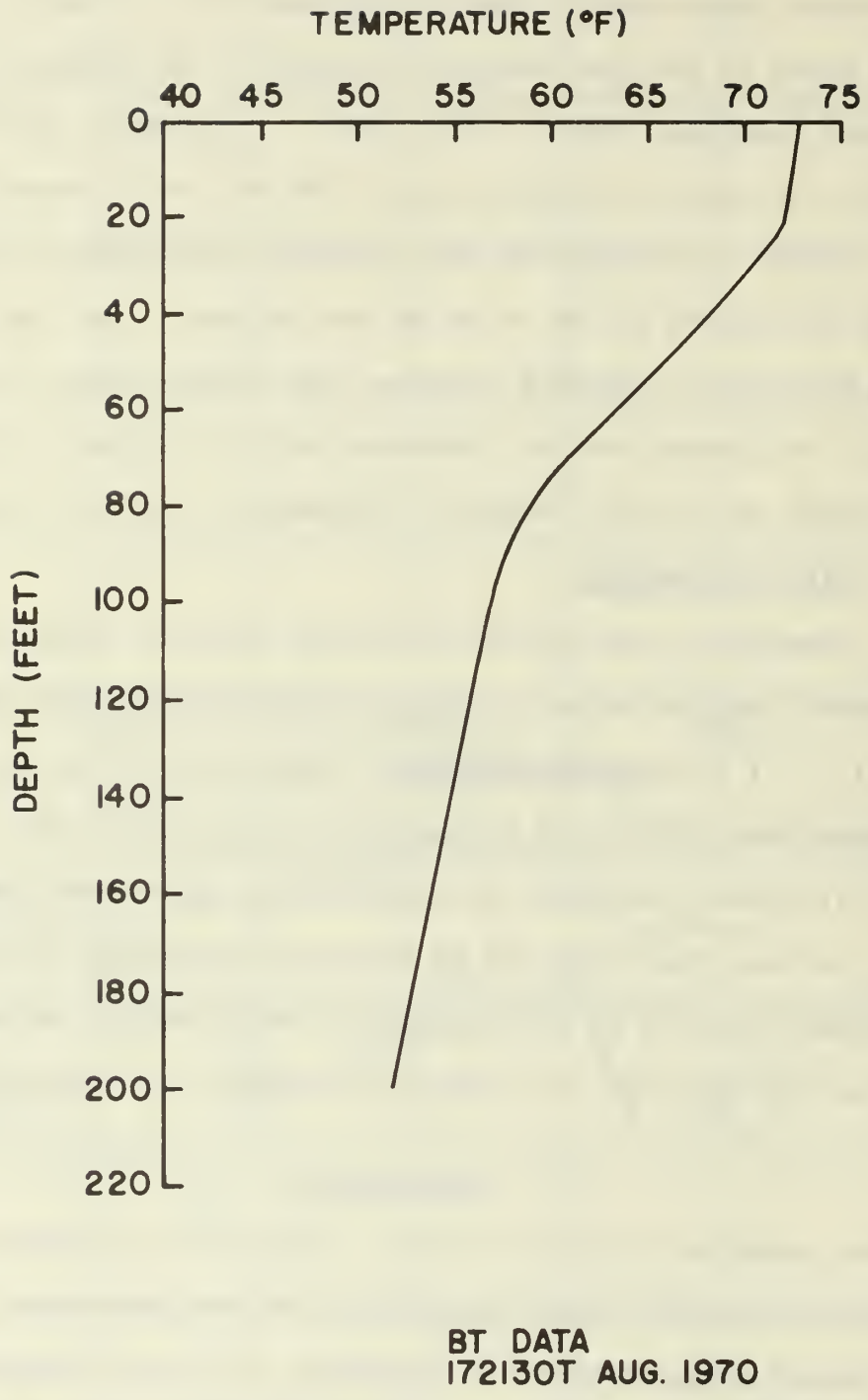

Figure 26. Bathythermograph at time of experiments.

factor e^{-R}. For larger acoustical roughnesses, $R \geq 1$, it is possible to make predictions that come close to reality provided the ensonified surface is judiciously divided into sub-areas. The experimental data are not able to clearly demonstrate the presence of an important lateral wave component for low roughness surfaces.

Greater accuracy for the rough surface transmission problem will require a theoretical approach that takes into account the lateral wave in the case of a rough surface and which considers interactions between sub-areas or deals with the affects of diverging waves from the beginning of the development.

REFERENCES

1. H. Medwin and J.D. Hagy, Jr., "Helmholtz-Kirchhoff Theory for Sound Transmission Through a Statistically-Rough Plane Interface Between Dissimilar Fluids", J. Acoust. Soc. Am. 51, 1083-1090 (1972).

2. C.W. Horton, Sr., and D.R. Melton, "Importance of the Fresnel Correction in Scattering from a Rough Surface II", J. Acoust. Soc. Am. 47, 299-303 (Jan. 1970); see also Part I by same authors, same issue pp. 290-298.

3. B.E. Parkins, "Reflection and Scattering from a Time-Varying Rough Surface - the Nearly Complete Lloyd's Mirror Effect", J. Acoust. Soc. Am. 49, 1484-1490 (May 1971).

4. P. Beckman and A. Spizzichino, The Scattering of Electromagnetic Waves from Rough Surfaces, (Macmillan, New York, 1963).

5. I. Tolstoy and C.S. Clay, Ocean Acoustics, Theory and Experiment in Underwater Sound, (McGraw Hill, New York, 1966).

6. H. Medwin, "Ch. 3, Scattering from the Sea Surface" in Underwater Acoustics, ed. by R.W.B. Stephens (Wiley-Interscience, London and New York, 1970).

7. C.S. Clay and H. Medwin, "Dependence of Spatial and Temporal Correlation of Forward-Scattered Underwater Sound on the Surface Statistics I. Theory," J. Acoust. Soc. Am. 47, 1412-1418 (May 1970).

8. James Dixon Hagy, Jr., "Transmission of Sound Through a Randomly Rough Air-Sea Interface", Electrical Engineer Thesis, Naval Postgraduate School, Monterey, California 93940, Sept. 1970.

9. John F. Waters, "Measurement of Transmission and Penetration of Airborne Explosive Sound into a Body of Water", J. Acoust. Soc. Am. 50, 102(A), 1971.

10. Robert W. Young, "Sound Pressure in Water from a Source in Air", J. Acoust. Soc. Am. 50, 1392(L), (1971).

11. Raymond Allan Helbig, "The Effects of Ocean Surface Roughness on the Transmission of Sound from an Airborne Source", M.S. Thesis, Naval Postgraduate School, Monterey, California 93940, Dec 1970.

12. J.R. Wilson, N.E.J. Boston, and W.W. Denner, Naval Postgraduate School Report Serial NPS-58DW9071A, Digital Analysis of Turbulence Data on the IBM 360/67 at the Naval Postgraduate School.

13. E. Gerjuoy, "Refraction of Waves from a Point Source into a Medium of Higher Velocity", Phys. Rev. 73, 1442-1449 (1948).

14. L. Brekhovskikh, "Waves in Layered Media", (Academic Press, N.Y. 1960).

INITIAL DISTRIBUTION LIST

		No. of Copies
1.	ASW Systems Project Office, Code ASW21 Navy Department Washington, D.C. 20360	2
2.	ASW Systems Project Office, Code ASW24 Navy Department Washington, D.C. 20360	2
3.	Office of Naval Research (Code 468) Department of the Navy Arlington, Virginia 22217	2
4.	Director, Naval Research Laboratory Technical Information Division Department of the Navy Washington, D.C. 20390	3
5.	Director, Advanced Research Projects Agency Technical Library, The Pentagon Washington, D.C. 20301	3
6.	Defense Documentation Center Cameron Station Alexandria, Virginia 22314	12
7.	Commanding Officer Office of Naval Research Branch Office 219 S. Dearborn Street Chicago, Illinois 60604	1
8.	Commanding Officer Office of Naval Research Branch Office 1030 East Green Street Pasadena, California 91101	1
9.	Commanding Officer Office of Naval Research Branch Office 495 Summer Street Boston, Massachusetts 02210	1
10.	San Francisco Area Office Office of Naval Research 1076 Mission Street San Francisco, California 94109	1
11.	New York Area Office Office of Naval Research 207 W. 24th Street New York, New York 10011	1

12. Director — 2
Naval Research Laboratory
Library, Code 2029 (ONRL)
Washington, D.C. 20390

13. Commander — 1
Naval Ordnance Laboratory
Acoustics Division
White Oak, Silver Spring, Maryland 20910

14. Commander — 1
Navy Undersea Research & Development Center
Technical Library
San Diego, California 92152

15. Officer-in-Charge — 1
Technical Library
Naval Underwater Systems Center
Newport, Rhode Island 02840

16. Commanding Officer — 1
Technical Library
Naval Underwater Systems Center
Fort Trumbull, New London, Connecticut 06321

17. Naval Ship Research & Development Center — 1
Central Library
Washington, D.C. 20034

18. Commanding Officer — 1
Naval Air Development Center
Johnsville, Warminster, Pennsylvania 18974

19. Commanding Officer — 1
Navy Mine Defense Laboratory
Panama City, Florida 32402

20. Naval Research Laboratory — 1
Underwater Sound Reference Division
Technical Library
P.O. Box 8337
Orlando, Florida 32806

21. Naval Weapons Center — 1
Technical Library
China Lake, California 93555

22. Naval Undersea Warfare Center — 1
Technical Library
3202 E. Foothill Boulevard
Pasadena, California 91107

23. Office of the Director of Defense Research and Engineering
Information Office Library Branch
The Pentagon
Washington, D.C. 20301 — 1

24. U.S. Army Research Office
Box CM, Duke Station
Durham, North Carolina 27706 — 1

25. Air Force Office of Scientific Research
Department of the Air Force
Washington, D.C. 20333 — 1

26. Air Force Avionics Laboratory
Air Force Systems Command
Technical Library
Wright-Patterson Air Force Base
Dayton, Ohio 45433 — 1

27. Naval Postgraduate School
Technical Library
Monterey, California 93940 — 1

28. Naval Academy
Technical Library
Annapolis, Maryland 21401 — 1

29. Research & Technology Directorate
Naval Electronics Systems Command
Department of the Navy
Washington, D.C. 20360 — 1

30. RDT&E Planning Division
Naval Ship Systems Command
Department of the Navy
Washington, D.C. 20360 — 1

31. Research and Technology
Naval Air Systems Command
Department of the Navy
Washington, D.C. 20360 — 1

32. Research and Technology Directorate
Naval Ordnance Systems Command
Department of the Navy
Washington, D.C. 20360 — 1

33. Office of Naval Research
Code 461
Department of the Navy
Arlington, Virginia 22217 — 1

34. Attn: Dr. John F. Waters — 1
Hydrospace Research Corporation
2150 Fields Road
Rockville, Maryland 20850

35. General Electric Company — 1
Mr. R.J. Twardzik
Court Street, Plant No. 9
Syracuse, New York 13201

36. Mr. R.J. Urick — 1
Research Acoustics Division
U.S. Naval Ordnance Laboratory
Silver Spring, Maryland 20910

37. Mr. I. Sochard — 1
U.S. Naval Ordnance Laboratory
Silver Spring, Maryland 20910

38. Mr. R.W. Young — 1
Naval Undersea Research & Development Center
San Diego, California 92132

39. Dr. A.A. Hudimac — 1
Scientific Research Associates, Inc.
12100 Devilwood Drive
Potomac, Maryland 20854

40. Lt. D.H. Bennet — 1
U.S. Naval Ship Systems Command
Department of the Navy
Washington, D.C. 20360

41. Dr. M.S. Weinstein — 1
Underwater Systems, Inc.
8121 Georgia Avenue
Silver Spring, Maryland 20910

42. Mr. Glenn Elmer — 1
U.S. Naval Ship Research & Development Center
Washington, D.C. 20034

43. Mr. D.A. Hilton — 1
National Aeronautics & Space Administration
Langley Research Center
Hampton, Virginia 23365

44. Mr. John Bellino — 1
U.S. Naval Air Systems Command
Department of the Navy
Washington, D.C. 20360

45. Dr. D. Bordelon — 1
Naval Underwater Systems Center
Newport, Rhode Island 02840

46. Mr. J. Conrad — 1
U.S. Naval Scientific & Technical Intelligence Center
4301 Suitland Road
Suitland, Maryland 20023

47. Mr. L. Freeman — 1
Naval Underwater Systems Center
New London, Connecticut 06320

48. Dr. J. Macaluso — 1
Ordnance Research Laboratory
Penn State University
University Park, Pennsylvania 16801

49. Dr. J.C. Munson — 1
U.S. Naval Research Laboratory
Washington, D.C. 20390

50. Dr. H. Medwin, Code 61Md — 10
Naval Postgraduate School
Monterey, California 93940

51. Mr. E. Wynnuzzi — 1
U.S. Naval Air Development Center
Johnsville, Pennsylvania 18974

52 Mr. Donald Rothacker — 1
Riverside Research Institute
80 West End Avenue
New York, New York 10023

53. Mr. R. Uranicar (Code 370E) — 1
Naval Air Systems Command
Department of the Navy
Washington, D.C. 20360

54. Sonar Directorate (Ships 901) — 1
Naval Ship Systems Command
Department of the Navy
Washington, D.C. 20360

55. Acoustic Warfare Project (PMS-394) — 1
Naval Ship Systems Command
Department of the Navy
Washington, D.C. 20360

56. LT J.H. Hagy — 1
Fairkef
US Naval Station, Keflavik
APO New York 09571

57. LCDR R.A. Helbig 1
USS NOA DD841
APO New York 09501

58. Dr. W.F. Hunter, Superintendent 1
RAN Research Laboratory
Golden Island
New South Wales, Australia 2000

59. Dr. G. Gaunaurd 1
Acoustics Division
Naval Ordnance Lab
White Oak
Silver Spring, Maryland 20910

60. Prof. C.S. Clay 1
Dept. of Geology & Geophysics
Geophysical & Polar Research Center
University of Wisconsin
Middleton, Wisconsin 53562

61. Dr. John Wood 1
Admiralty Underwater Weapons Estab.
Portland, Dorset
England

62. Dr. John McDoy 1
Naval Research Laboratory
Washington, D.C. 20390

63. Dr. A.G. Fabula, Code 2542 1
Naval Undersea Research & Development Center
3202 E. Foothill Bldvd.
Pasadena, California 91107

64. Dr. Eric Risness 1
Admiralty Underwater Weapons Estab.
Portland, Dorset
England

65. John C. Calhoun 1
Department of Physics
Naval Postgraduate School
Monterey, California 93940

66. C.E. Menneken 1
Dean of Research Administration
Naval Postgraduate School
Monterey, California 93940

DOCUMENT CONTROL DATA - R & D

(Security classification of title, body of abstract and indexing annotation must be entered when the overall report is classified)

1. ORIGINATING ACTIVITY (Corporate author)
Naval Postgraduate School
Monterey, California 93940

2a. REPORT SECURITY CLASSIFICATION
Unclassified

2b. GROUP

3. REPORT TITLE
Frequency Dependence of Sound Transmitted From An Airborne Source Into the Ocean

4. DESCRIPTIVE NOTES (Type of report and inclusive dates)
Technical Report, NPS-61Md72051A, 15 May 1972

5. AUTHOR(S) (First name, middle initial, last name)
Herman Medwin & R.A. Helbig

6. REPORT DATE
May 1972

7a. TOTAL NO. OF PAGES
59

7b. NO. OF REFS
14

8a. CONTRACT OR GRANT NO.

b. PROJECT NO.

c.

d.

9a. ORIGINATOR'S REPORT NUMBER(S)

9b. OTHER REPORT NO(S) (Any other numbers that may be assigned this report)

10. DISTRIBUTION STATEMENT
Approved for public release; distribution unlimited.

11. SUPPLEMENTARY NOTES

12. SPONSORING MILITARY ACTIVITY
Naval Postgraduate School
Monterey, California 93940

13. ABSTRACT

The predicted dependence of sound transmission on the statistics of the randomly-rough interface between dissimilar fluids has been studied by use of the Helmholtz Integral (J. Acoust. Soc. Amer. 51, 1083-1090 (1972). The predictions have been verified for radiation from a helicopter hovering, and slowly moving, over the sea, for frequencies to 1000 Hz for a wide range of surface acoustical roughnesses, $R = k_2^2\sigma^2[(c_2/c_1)\cos\theta_1 - \cos\theta_2]^2$. The roughness parameters σ,k,c and θ are the rms height of the surface, propagation constant, speed of propagation and angle with the normal, respectively; subscript 1 refers to air and 2 to the water.

When the surface is mirror-smooth, the transmitted sound pressure is due to the change in divergence and change in impedance at the interface. For low roughness, $R < 1$, the mean square transmitted pressure becomes decreasingly coherent and is a function of frequency; its magnitude is decreased by the factor e^{-R} compared to the perfectly smooth surface. For $R \geq 1$ the incoherent component dominates and the transmitted pressure depends also on the correlation length of the surface displacements.

The transmission change of sound pressure as a function of frequency is presented for several conditions of an SH3-D helicopter hovering and flying over or near an array of microphone and sonobuoy hydrophones.

14 KEY WORDS	LINK A		LINK B		LINK C	
	ROLE	WT	ROLE	WT	ROLE	WT
Sound Refraction						
Rough-Surface Transmission						